Prevailing climatic trends and runoff response from Hindukush-Karakoram-Himalaya, upper Indus basin

S. Hasson[1,2], J. Böhner[1], V. Lucarini[2,3]

[1] CEN, Centre for Earth System Research and Sustainability, Institute for Geography, University of Hamburg, Hamburg, Germany

[2] CEN, Centre for Earth System Research and Sustainability, Meteorological Institute, University of Hamburg, Hamburg, Germany

[3] Department of Mathematics and Statistics, University of Reading, Reading, UK

Correspondence to: S. Hasson (shabeh.hasson@uni-hamburg.de)

Abstract

Largely depending on meltwater from the Hindukush-Karakoram-Himalaya, withdrawals from the upper Indus basin (UIB) contribute to half of the surface water availability in Pakistan, indispensable for agricultural production systems, industrial and domestic use and hydropower generation. Despite such importance, a comprehensive assessment of prevailing state of relevant climatic variables determining the water availability is largely missing. Against this background, we present a comprehensive hydroclimatic trend analysis over the UIB. We analyze trends in maximum, minimum and mean temperatures (Tx, Tn, and Tavg, respectively), diurnal temperature range (DTR) and precipitation from 18 stations (1250-4500 m asl) for their overlapping period of record (1995-2012), and separately, from six stations of their long term record (1961-2012). We apply Mann-Kendall test on serially independent time series to assess existence of a trend while true slope is estimated using Sen's slope method. Further, we statistically assess the spatial scale (field) significance of local climatic trends within ten identified sub-regions of the UIB and analyze whether spatially significant (field significant) climatic trends qualitatively agree with a trend in discharge out of corresponding sub-regions. Over the recent period (1995-2012), we find a well agreed and mostly field significant cooling (warming) during monsoon season i.e. July-October (March-May and November), which is higher in magnitude relative to long term trends (1961-2012). We also find a general cooling in Tx and a mixed response of Tavg during winter season as well as a year round decrease in DTR, which is stronger and more significant at high altitude stations (above 2200 m asl), and mostly due to higher cooling in Tx than in Tn. Moreover, we find a field significant decrease (increase) in late-monsoonal precipitation for lower (higher) latitudinal regions of Himalayas (Karakoram and Hindukush), whereas an increase in winter precipitation for Hindukush, western- and whole Karakoram, UIB-Central, UIB-West, UIB-West-upper and whole UIB regions. We find a spring warming (field significant in March) and drying (except for Karakoram and its sub-regions), and subsequent rise in early-melt season flows. Such early melt response together with effective cooling during monsoon period subsequently resulted in a substantial drop (weaker increase) in discharge out of higher (lower) latitudinal regions (Himalaya and UIB-West-lower) during late-melt season, particularly during July. The observed hydroclimatic trends, being driven by certain changes in the monsoonal system and westerly disturbances, indicate dominance (suppression) of nival (glacial) runoff regime, altering substantially the overall hydrology of the UIB in future. These findings largely contribute to address the hydroclimatic explanation of the 'Karakoram Anomaly'.

1 Introduction

The hydropower generation has key importance in minimizing the on-going energy crisis in Pakistan and meeting country's burgeoning future energy demands. In this regard, seasonal water availability from the upper Indus basin (UIB) that contributes to around half of the annual average surface water availability in Pakistan is indispensable for exploiting 3500 MW of installed hydropower potential at country's largest Tarbela reservoir immediate downstream. This further contributes to the country's agrarian economy by meeting extensive irrigation water demands. The earliest water supply from the UIB after a long dry period (October to March) is obtained from melting of snow (late-May to late-July), the extent of which largely depends upon the accumulated snow amount and concurrent temperatures (Fowler and Archer, 2005; Hasson et al., 2014b). Snowmelt runoff is then overlapped by glacier melt runoff (late-June to late-August), primarily depending upon the melt season temperatures (Archer, 2003). Snow and glacier melt runoffs, originating from the Hindukush-Karakoram-Himalaya (HKH) Ranges, together constitute around 70-80% of the mean annual water available from the UIB (SIHP, 1997; Mukhopadhyay and Khan, 2015; Immerzeel et al., 2009). As opposed to large river basins of South and Southeast Asia, which feature extensive summer monsoonal wet regimes downstream, the lower Indus basin is mostly arid and hyper-arid and much relies upon the meltwater from the UIB (Hasson et al., 2014b).

Climate change is unequivocal and increasingly serious concern due to its apparent recent acceleration. For instance, the last three decades have been the warmest at a global scale since 1850, while the period of 1983-2012 in the Northern Hemisphere has been estimated as the warmest since last 1400 years (IPCC, 2013). The global warming signal, however, is spatially heterogeneous and not necessarily equally significant across different regions (Yue and Hashino, 2003; Falvey and Garreaud, 2009). Similarly, local impacts of the regionally varying climate change can differ substantially, depending upon the local adaptive capacity, exposure and resilience (Salik et al., 2015), particularly for the sectors of water, food and energy security. In view of high sensitivity of mountainous environments to climate change and the role of meltwater as an important control for the UIB runoff dynamics, it is crucial to assess the prevailing climatic state over the UIB and subsequent water availability. Several studies have been performed in this regard. For example, Archer and Fowler (2004) have analyzed trends in precipitation from four stations within the UIB and found a significant increase in winter, summer and annual precipitation during the period 1961-1999. By analyzing temperature trends for the same period, Fowler and Archer (2006) have found a significant cooling in summer and warming in winter. Sheikh et al. (2009) documented a significant cooling of mean temperatures during the monsoon period (July-September), and consistent warming during the pre-monsoonal months (April-May) for the period 1951-2000. They have found a significant increase in monsoonal precipitation while non-significant changes for the rest of year. Khattak et al. (2011) have found winter warming, summer cooling (1967-2005), but no definite pattern for precipitation. It is noteworthy that reports from the above mentioned studies are based upon at least a decade old data records. Analyzing updated data for the last three decades (1980-2009), Bocchiola and Diolaiuti (2013) have suggested that winter warming and summer cooling trends are less general than previously thought, and can be clearly assessed only for Gilgit and Bunji stations, respectively. For precipitation, they found an increase over the Chitral-Hindukush and northwest Karakoram regions and decrease over the Greater Himalayas within the UIB, though most of such precipitation changes are statistically insignificant. By analyzing temperature record for the period 1952-2009, Río et al. (2013) also reported dominant warming during March and pre-monsoonal period, consistent with findings of Sheikh et al. (2009).

The above mentioned studies have analyzed observations from only a sub-set of half dozen manual, valley-bottom, low-altitude stations being maintained by Pakistan Meteorological

Department (PMD) within the UIB (Hasson et al., 2014b). Contrary to these low-altitude stations, observations from high altitude stations in South Asia mostly feature opposite sign of climatic changes and extremes, possibly influenced by the local factors (Revadekar et al., 2013). Moreover, the bulk of the UIB streamflow originates from the active hydrologic zone (2500-5500 m asl), when thawing temperatures migrate over and above 2500 m asl (SIHP, 1997). In view of such a large altitudinal dependency of the climatic signals, data from low-altitude stations, though extending back into the first half of 20th century, are not optimally representative of the hydro-meteorological conditions prevailing over the UIB frozen water resources (SIHP, 1997). Thus, an assessment of climatic trends over the UIB has been much restricted by limited availability of high-altitude and most representative observations as well as their accessibility, so far.

Amid above mentioned studies, Archer and Fowler (2004), Fowler and Archer (2006) and Sheikh et al. (2009) have used linear least square method for trend analysis. Though such parametric tests more robustly assess the existence of a trend as compared to non-parametric trend tests (Zhai et al., 2005), they need the sample data to be normally distributed, which is not always the case for hydro-meteorological observations (Hess et al., 2001; Khattak et al., 2011). In this regard a non-parametric test, such as, Mann Kendall (MK - Mann, 1945; Kendall, 1975) is a pragmatic choice, which has been extensively adopted for the hydro-climatic trend analysis (Kumar et al., 2009 and 2013). The above mentioned studies of Khattak et al. (2011), Río et al. (2013) and Bocchiola and Diolaiuti (2013) have used MK test in order to confirm the existence of a trend along with Theil-Sen (TS - Theil, 1950; Sen, 1968) slope method to estimate true slope of a trend.

Most of the hydro-climatic time series contain red noise because of the characteristics of natural climate variability, and thus, are not serially independent (Zhang et al., 2000; Yue et al., 2002 & 2003; Wang et al., 2008). On the other hand, MK statistics is highly sensitive to serial dependence of a time series (Yue and Wang, 2002; Yue et al., 2002 & 2003; Khattak et al., 2011). For instance, the variance of MK statistic S increases (decreases) with the magnitude of significant positive (negative) auto-correlation of a time series, which leads to an overestimation (underestimation) of trend detection probability (Douglas et al., 2000; Yue et al., 2002 and 2003; Wu et al., 2008; Rivard and Vigneault, 2009). To eliminate such an effect, von Storch (1995) and Kulkarni and von Storch (1995) proposed a pre-whitening procedure that suggests the removal of a lag-1 auto-correlation prior to applying the MK-test.

Río et al. (2013) have analyzed trends using pre-whitened (serially independent) time series. This procedure, however, is particularly inefficient when a time series features a trend or it is serially dependent negatively (Rivard and Vigneault, 2009). In fact, presence of a trend can lead to false detection of significant positive (negative) auto-correlation in a time series (Rivard and Vigneault, 2009), removing which through pre-whitening procedure may remove (inflate) the portion of a trend, leading to an underestimation (overestimation) of trend detection probability and trend magnitude (Yue and Wang, 2002; Yue et al., 2003). In order to address this problem, Yue et al. (2002) have proposed a modified pre-whitening procedure, which is called trend free pre-whitening (TFPW). In TFPW, a trend component is separated before the pre-whitening procedure is applied, and after the pre-whitening procedure, the resultant time series is blended together with the pre-identified trend component for further application of the MK test. Khattak et al. (2011) have applied TFPW to make time series serially independent before trends analysis. The TFPW method takes an advantage of the fact that estimating auto-correlation coefficient from a detrended time series yields its more accurate magnitude for the pre-whitening procedure (Yue et al., 2002). However, prior estimation of a trend may also be influenced by the presence of a serial correlation in a time series in a similar way the presence of a trend contaminates estimates of an auto-correlation coefficient (Zhang et al., 2000). It is, therefore, desirable to estimate most accurate magnitudes of both, trend and auto-correlation coefficient, in order to avoid the influence of one on the other.

The UIB observes contrasting hydro-meteo-cryospheric regimes mainly because of the complex HKH terrain and sophisticated interaction of prevailing regional circulations (Hasson et al., 2014a and 2015a). The sparse (high and low altitude) meteorological network in such a difficult area neither covers fully its vertical nor its horizontal extent - it may also be highly influenced by complex terrain features and variability of meteorological events. Under such scenario, tendencies ascertained from the observations at local sites further need to be assessed for their field significance. The field significance indicates whether the stations within a particular region collectively exhibit a significant trend or not, irrespective of the significance of individual trends (Vogel and Kroll, 1989; Lacombe and McCarteny, 2014). This yields a dominant signal of change and much clear understanding of what impacts the observed conflicting climate change will have on the overall hydrology of the UIB and of its sub-regions. However, similar to sequentially dependent local time series, spatial-/cross-correlation amid station network within a region, possibly present due to the influence of a common climatic phenomenon and/or of similar physio-geographical features (Yue and Wang, 2002), anomalously increases the probability of detecting field significant trends (Yue et al., 2003; Lacombe and McCarteny, 2014). Such effect of cross/spatial correlation amid station network should be eliminated while testing the field significance as proposed by several studies (Douglas et al., 2000; Yue and Wang, 2002; Yue et al., 2003)

In this study, we present a first comprehensive and systematic hydro-climatic trend analysis for the UIB based upon ten stream flow, six low altitude manual and 12 high-altitude automatic weather stations. We apply a widely used non-parametric MK trend test over serially independent time series, obtained through a pre-whitening procedure, for ensuring the existence of a trend. The true slope of an existing trend is estimated by the Sen's slope method. In pre-whitening, we remove negative/positive lag-1 autocorrelation that is optimally estimated through an iterative procedure, so that, pre-whitened time series feature the same trend as of original time series. Here, we investigate climatic trends on monthly time scale in addition to seasonal and annual time scales, first in order to present a more comprehensive picture and secondly to circumvent the loss of intra-seasonal tendencies due to an averaging effect. For assessing the field significance of local climatic trends, we divide the UIB into ten regions, considering its diverse hydrologic regimes, HKH topographic divides and installed hydrometric station network. Such regions are Astore, Hindukush (Gilgit), western-Karakoram (Hunza), Himalaya, Karakoram, UIB-Central, UIB-West, UIB-West-lower, UIB-West-upper and the UIB itself (Figs. 1-2). Provided particular region abodes more than one meteorological station, individual climatic trends within that region were tested for their field significance based upon the number of positive/negative significant trends (Yue et al., 2003). Field significant trends are in turn compared qualitatively with trends of outlet discharge from the corresponding regions, in order to furnish physical attribution to statistically identified regional signal of change. Our results, presenting prevailing state of the hydro-climatic trends over the HKH region within the UIB, contribute to the hydroclimatic explanation of the 'Karakoram Anomaly', provide right direction for the impact assessment and modelling studies, and serve as an important knowledge base for the water resource managers and policy makers in the region.

2 Upper Indus basin

The UIB is a unique region featuring complex HKH terrain, distinct physio-geographical features, conflicting signals of climate change and subsequently contrasting hydrological regimes (Archer, 2003; Fowler and Archer, 2006; Hasson et al., 2013). The basin extending from the western Tibetan Plateau in the east to the eastern Hindu Kush Range in the west hosts mainly the Karakoram Range in the north, and western Himalayan massif (Greater Himalaya) in the south (Fig. 1). As summarized in Reggianni and Rientjes (2014) and Khan et al. (2014), the total drainage area of the UIB has long been overestimated by various studies (e.g. Immerzeel et al., 2009; Tahir, 2011; Bookhagen and Burbank, 2010). Such overestimation is caused by limitations of the GIS-based automated watershed-delineation procedure that results in erroneous inclusion of the Pangong Tso watershed (Khan et al., 2014), which instead is a closed basin (Huntington, 1906; Brown et al., 2003, Alford, 2011). Khan et al. (2014) have provided details about the delineation of the UIB based upon ASTER GDEM 30m and SRTM 90m DEMs. For this study, the UIB drainage area is estimated from the lately available 30 meter version of the SRTM DEM, which was forced to exclude the area connecting the UIB to the Pangong Tso watershed in order to avoid its erroneous inclusion by the applied automated delineation procedure. Details of the delineation procedure will be provided elsewhere. Our estimated area of the UIB at Besham Qila is around 165515 km^2, which is to a good approximation consistent with the actual estimates of 162393 km^2 as reported by the SWHP, WAPDA. According to the newly delineated basin boundary, the UIB is located within the geographical range of 31-37^o E and 72-82^o N. Around 46 % of the UIB falls within the political boundary of Pakistan, containing around 60 % of the permanent cryospheric extent. Based on the Randolph Glacier Inventory version 5.0 (RGI5.0 - Arendt et al., 2015), around 12% of the UIB area (19,370 km^2) is under the glacier cover. While snow cover ranges from 3 to 67% of the basin area (Hasson et al., 2014b).

The hydrology of the UIB is dominated by precipitation regime associated with the mid-latitude western disturbances. These western disturbances are lower-tropospheric extra-tropical cyclones, which are originated and/or reinforced over the Atlantic Ocean or the Mediterranean and Caspian Seas and transported over the UIB by the southern flank of the Atlantic and Mediterranean storm tracks (Hodges et al., 2003; Bengtsson et al., 2006). The western disturbances intermittently transport moisture over the UIB mainly in solid form throughout the year, though their main contribution comes during winter and spring (Wake, 1989; Rees and Collins, 2006; Ali et al., 2009; Hewitt, 2011; Ridley et al., 2013; Hasson et al., 2013 & 2015a). Such contributions are anomalously higher during positive phase of the north Atlantic oscillation (NAO), when southern flank of the western disturbances intensifies over Iran and Afghanistan because of heat low there, causing additional moisture input to the region from the Arabian Sea (Syed et al., 2006). Similar positive precipitation anomaly is evident during warm phase of the El Niño–Southern Oscillation (ENSO - Shaman and Tziperman, 2005; Syed et al., 2006). In addition to westerly precipitation, the UIB also receives contribution from the summer monsoonal offshoots, which crossing main barrier of the Greater Himalayas (Wake, 1989; Ali et al., 2009; Hasson et al., 2015a), precipitate moisture over higher (lower) altitudes in solid (liquid) form (Archer and Fowler, 2004). Such occasional incursions of the monsoonal system and the dominating westerly disturbances, largely controlled by the complex HKH terrain, define contrasting hydro-climatic regimes within the UIB. Mean annual precipitation within the UIB ranges from less than 150 mm at Gilgit station to around 700 mm at Naltar station. Lately, addressing precipitation uncertainty over the whole UIB, Immerzeel et al. (2015) have suggested the amount of precipitation more than twice as previously thought. The glaciological studies also suggest substantially large amount of snow accumulation that account for 1200-1800 mm (Winiger et al., 2005) in Bagrot valley and above 1000 mm over the Batura Glacier (Batura Investigation Group, 1979) within the western Karakoram, and more than 1000 mm and, at few sites above 2000 mm over the Biafo and Hispar glaciers (Wake, 1987) within the central Karakoram.

The Indus River and its tributaries are gauged at ten key locations within the UIB, dividing it into Astore, Gilgit, Hunza, Shigar and Shyok sub-basins (Fig. 2). These basins feature distinct hydrological regimes (snow- and glacier-fed). Previous studies (Archer 2003; Mukhopadhyay and Khan, 2015) have separated snow-fed (glacier-fed) sub-basins of the UIB on the basis of their; 1) smaller (larger) glacier coverage, 2) strong runoff correlation with previous winter precipitation (concurrent temperatures) from low altitude stations, and, 3) using hydrograph separation technique. Based on such division, Astore (within the western Himalayan Range) and Gilgit (within the eastern Hindukush Range) are considered as mainly snow-fed while Hunza, Shigar and Shyok (within the Karakoram Range) are considered as mainly glacier-fed sub-basins. The strong influence of climatic variables on the generated runoff within and from the UIB suggests vulnerability of spatio-temporal water availability to climatic changes. This is why the UIB discharge features high variability – the maximum mean annual discharge is around an order of magnitude higher than its minimum mean annual discharge, in extreme cases. Mean annual discharge from the UIB is around 2400 m^3s^{-1}, which contributes to around 45 % of the total surface water availability within Pakistan. Since the

UIB discharge contribution is dominated by snow and glacier melt, it concentrates mainly within the melt season (April – September). During the rest of year, melting temperatures remain mostly below the active hydrologic elevation range, resulting in minute melt runoff (Archer, 2004). The characteristics of the UIB and its sub-basins are summarized in Table 1.

3 Data

3.1 Meteorological data

The network of meteorological stations within the UIB is very sparse and mainly limited to within Pakistan's political boundaries, where around 20 meteorological stations are being operated by three different organizations. The first network, operated by PMD, consists of six manual valley-based stations that provide the only long-term data series, generally starting from first half of the 20th century. However, data before 1960 are scarce and feature large data gaps (Sheikh et al., 2009). Such dataset covers a north-south extent of around 100 km from Gupis to Astore station and east-west extent of around 200 km from Skardu to Gupis station. These stations lie within the western Himalaya and Hindukush ranges and between the altitudinal range of 1200-2200 m asl, whereas most of the ice reserves of the Indus Basin lie within the Karakoram range (Hewitt, 2011) and above 2200 m asl (Fig. 1). In the central Karakoram, EvK2-CNR has installed two meteorological stations at higher elevations, which however, provide time series only since 2005. Moreover, the precipitation gauges within PMD and EvK2-CNR networks measure only liquid precipitation, while the hydrology of the region is dominated by solid moisture melt. The third meteorological network within the UIB consists of 12 high altitude automatic weather stations, called Data Collection Platforms (DCPs), which are being maintained by the Snow and Ice Hydrology Project (SIHP) of WAPDA. The DCP data is being observed at hourly intervals and is transferred to the central SIHP office in Lahore on a real time basis through a Meteor-Burst communication system. The data is subject to missing values due to rare technical problems, such as 'sensor not working' and/or 'data not received from broadcasting system'. Featuring higher altitude range of 1479-4440 m asl, these DCP stations provide meteorological observations since 1994/95. Contrary to PMD and EvK2-CNR, precipitation gauges at DCPs measure both liquid and solid precipitation in mm water equivalent (Hasson et al., 2014b). Moreover, DCPs cover relatively larger spatial extent, such as, north-south extent of 200 km from Deosai to Khunjrab stations and east-west extent of around 350 km from Hushe to Shendure stations.

Thus, spreading well across the HKH ranges and covering most of the active hydrologic zone, DCPs seem to be well representative of the prevailing hydro-meteorological conditions over the UIB cryosphere, so far. We have collected daily data for maximum and minimum temperatures (Tx and Tn, respectively) and precipitation of 12 DCPs for the period 1995-2012 from SIHP, WAPDA (Table 2). We have also collected the updated record of six low altitude stations from PMD for same set of variables within the period 1961-2012.

3.2 Discharge data

The discharge data, being highly sensitive to variations in precipitation, evaporation, basin storage and prevailing thermal regime, describe the overall hydrology and an integrated signal of hydrologic change for a particular watershed. In order to provide physical attribution to our statistically based field significant trend analysis, we have collected the discharge data from SWHP, WAPDA. The project maintains a network of hydrometric stations within Pakistan. The upper Indus river flows are being measured first at Kharmong site where the Indus river enters into Pakistan and then at various locations until it enters into the Tarbela reservoir. The river inflows measuring stations at Tarbela reservoir, and few kilometers above it, at the Besham Qila are usually considered to separate the upper part (i.e. UIB) from the rest of Indus basin. Five sub-basins are being gauged, among which Shigar gauge has not been operational since 2001. Since we take the UIB extent up to the Besham Qila site, we have collected full length of discharge data up to 2012 for all ten hydrometric stations within the UIB (Table 3). It is pertinent to mention here that discharge data from central and eastern parts of the UIB are hardly influenced by the anthropogenic perturbations. The western UIB is relatively populous and streamflow is used for solo-seasoned crops and domestic use, however, the overall water diversion for such a use is indeed negligible (Khattak et al., 2011).

4 Methods

Inhomogeneity in a climatic time series is due to variations ascribed purely to non-climatic factors (Conrad and Pollak, 1950), such as, changes in the station site, station exposure, observational methods, and measuring instruments (Heino, 1994; Peterson et al., 1998). Archer and Fowler (2004) and Fowler and Archer (2005 and 2006) have documented that PMD and WAPDA follow standard meteorological measurement practice established in 1891 by the Indian Meteorological Department. Using double mass curve approach, they have found inhomogeneity in the winter minimum temperature around 1977 only at Bunji station among four low altitude stations analyzed. Since climatic patterns are highly influenced by orographic variations and local events within the study region of complex terrain, double mass curve techniques may yield limited skill. Forsythe et al. (2014) have reported homogeneity of Gilgit, Skardu and Astore stations for annual mean temperature during the period 1961-1990 while Río et al. (2013) have reported homogeneity for temperature records from Gilgit, Gupis, Chillas, Astore and Skardu stations during 1952-2009. Some studies (Khattak et al., 2011; Bocchiola and Diolaiuti, 2013) do not report quality control or homogeneity of the data used for their analysis.

We have first investigated internal consistency of the data by closely following Klein Tank et al. (2009) such as situations of below zero precipitation and when maximum temperature was lower than minimum temperature, which found in few were then corrected. Afterwards, we have performed homogeneity tests using a standardized toolkit RH-TestV3 (Wang and Feng, 2009) that uses a penalized maximal F-test (Wang et al., 2008) to identify any number of change points in a time series. As no station has yet been reported homogenous at monthly time scale for all variables, only a relative homogeneity test is performed by adopting a most conservative threshold level of 99% for statistical significance. We have found mostly one inhomogeneity in only Tn for the low altitude PMD stations during the period of record, except for Skardu station (Table 2). For the 1995-2012 period, such inhomogeneity in Tn is only valid for Gilgit and Gupis stations. On the other hand, data from DCP stations were found of high quality and homogenous. Only Naltar station has experienced inhomogeneity in Tn during September 2010, which was most probably caused by heavy precipitation event resulted in a mega flood in Pakistan (Houze et al., 2011; Ahmad et al., 2012; Hasson et al., 2013) followed by similar events during 2011 and 2012. Since the history files were not available, we were not sure that any statistically found inhomogeneity only in Tn is real. Therefore, we did not apply any correction to inhomogeneous time series and caution the careful interpretation of results based on such time series.

4.1 Hydroclimatic trend analysis

We have analyzed trends in minimum, maximum and mean temperatures (Tn, Tx and Tavg, respectively), diurnal temperature range (DTR – Tx - Tn), precipitation and discharge on monthly to annual time scales. The MK test (Mann, 1945; Kendall, 1975) is applied to assess the existence of a trend while the Theil-Sen (TS - Theil, 1950; Sen, 1968) slope method is applied to estimate true slope of a trend. For sake of intercomparison between low and high altitude stations, we mainly analyze overlapping length of record (1995-2012) from high and low altitude stations, and additionally, the full length of record (1961-2012) from low altitude stations.

Mann-Kendall test

The MK is a ranked based method that tests the significance of an existing trend irrespective of the type of sample data distribution and whether such trend is linear or not (Yue et al., 2002; Wu et al., 2008; Tabari, H., and Talaee, 2011). Such test is also insensitive to the data outliers and missing values (Khattak et al., 2011; Bocchiola and Diolaiuti, 2013) and less sensitive to the breaks caused by inhomogeneous time series (Jaagus, 2006). The null hypothesis of the MK test states that the sample data $\{X_i, i = 1,2,3 \ldots n\}$ is independent and identically distributed, while alternative hypothesis suggests the existence of a monotonic trend. The MK statistics *S* are estimated as follows:

$$S = \sum_{i=1}^{n-1} \sum_{j=i+1}^{n} sgn\left(X_j - X_i\right) \qquad (1)$$

Where X_j denotes the sequential data, n denotes the data length, and

$$sgn(\theta) = \begin{cases} 1 & if\ \theta > 0 \\ 0 & if\ \theta = 0 \\ -1 & if\ \theta < 0 \end{cases} \qquad (2)$$

provided n ≥ 10, *S* statistics are approximately normally distributed with the mean, *E*, and variance, *V*, (Mann, 1945; Kendall, 1975) as follows:

$$E(S) = 0 \qquad (3)$$

$$V(S) = \frac{n(n-1)(2n+5) - \sum_{m=1}^{n} t_m m(m-1)(2m+5)}{18} \qquad (4)$$

Here, t_m denotes the number of ties of extent *m*, where tie refers to $\mathrm{X_j} = \mathrm{X_i}$. The standardized MK statistics, Z_s, can be computed as follows:

$$Z_s = \begin{cases} \frac{S-1}{\sqrt{V(S)}} & S > 0 \\ 0 & S = 0 \\ \frac{S+1}{\sqrt{V(S)}} & S < 0 \end{cases} \qquad (5)$$

The null hypothesis of no trend is rejected at a specified significance level, α, if $|Z_s| \geq Z_{a/2}$, where $Z_{\alpha/2}$ refers to a critical value of standard normal distribution with a probability of exceedance $\alpha/2$. The positive sign of Z shows an increasing while its negative sign shows a decreasing trend. We have reported the statistical significance of identified trends at 90, 95 and 99% levels by taking α as 0.1, 0.05 and 0.01, respectively.

Theil-Sen's slope estimation

Provided that a time series features a trend, it can be roughly approximated by a linear regression as

$$Y_t = a + \beta t + \gamma_t \qquad (6)$$

Where a is the intercept, β is the slope and γ_t is a noise process. Such estimates of β obtained through least square method are prone to gross errors and respective confidence intervals are sensitive to the type of parent distribution (Sen, 1968). We, therefore, have used Theil–Sen approach (TS - Theil, 1950; Sen, 1968) for estimating the true slope of existing trend as follows

$$\beta = Median\left(\frac{X_j - X_i}{j-i}\right), \forall\, i < j \qquad (7)$$

The magnitude of β refers to mean change of a variable over the investigated time period, while a positive (negative) sign implies an increasing (decreasing) trend.

Trend-perceptive pre-whitening (TPPW)

To pre-whiten the time series, we have used an approach of von Storch (1995) as modified by Zhang et al (2000). This approach iteratively computes trend and lag-1 auto-correlation until the solution converges to their most accurate estimates. This approach assumes that the trend can be approximated as linear (Eqn. 6) and the noise, γ_t, can be represented as a *p*th order auto-regressive process, AR(*p*) of the signal itself, plus the white noise, ε_t. Since the partial auto-correlations for lags larger than one are generally found insignificant (Zhang et al., 2000; Wang and Swail, 2001), considering only lag-1 auto-regressive processes, *r*, yields Eqn. 6 into:

$$Y_t = a + \beta t + rY_{t-1} + \varepsilon_t \qquad (8)$$

The iterative pre-whitening procedure consists of the following steps:

1. In first iteration, estimate of lag-1 autocorrelation, r_1 is computed on the original time series, Y_t.
2. Using r_1 as $(Y_t - r.Y_{t-1})\,/(1-r)$, an intermediately pre-whitened time series, $\acute{Y_t}$, is obtained on which first estimate of a trend, β_1 along with its significance is computed using TS (Theil, 1950; Sen, 1968) and MK (Mann, 1945; Kendall, 1975) methods.
3. The original time series, Y_t, is detrended using $\beta_1$as $(\widehat{Y_t} = Y_t - \beta_1 t)$.
4. In second iteration, more accurate estimate of lag-1 autocorrelation r_2 is estimated on detrended time series, $\widehat{Y_t}$, obtained from previous iteration.
5. The original time series Y_t, is again intermediately pre-whitened and $\acute{Y_t}$ is obtained.
6. The trend estimate β_2 is then computed on $\acute{Y_t}$ and the original time series, Y_t is detrended again, yielding $\hat{Y_t}$.

The procedure has to be reiterated until r is no longer significantly different from zero or the absolute difference between the estimates of r, β obtained from the two consecutive iterations becomes less than one percent. If any of the condition is met, let's suppose at the iteration *n*, estimates from the previous iteration (i.e. $r = r_{n-1}, \beta = \beta_{n-1}$) are taken as final. Using these final estimates, Eqn. 9 yields a pre-whitened time series, Y_t^w, which is serially independent and features the same trend as of original time series, Y_t (Zhang et al., 2000; Wang and Swail, 2001). Finally, the MK-test is applied over the pre-whitened time series, Y_t^w, to identify existence of a trend.

$$Y_t^w = \frac{(Y_t - r.Y_{t-1})}{(1-r)} = \hat{a} + \beta t + \epsilon_t \text{ , where } \hat{a} = a + \frac{r.\beta}{(1-r)} \text{ , and } \epsilon_t = \frac{\varepsilon_t}{(1-r)} \qquad (9)$$

4.2 Field significance and physical attribution

Field significance indicates when stations within a particular region collectively exhibit a significant trend, irrespective of the significance of individual trends (Vogel and Kroll, 1989; Lacombe and McCarteny, 2014). For assessing the field significance of local trends, we have divided the whole UIB into further smaller units/regions based on: 1) distinct hydrological regimes identified within the UIB, 2) mountain massifs, and, 3) available installed stream flow network.

As mentioned earlier, Shigar discharge time series is limited to 1985-2001 period since afterwards the gauge went non-operational. In order to analyze discharge trend from such an important region, Mukhopadhyay and Khan (2014) have first correlated the Shigar discharge with discharge from its immediate downstream Kachura gauge for the overlapping period of record (1985-1998). Then, they have applied the estimated monthly correlation coefficients to the post-1998 discharge at Indus at Kachura. This particular method can yield the estimated Shigar discharge, of course assuming that the applied coefficients remain valid after the year 1998. However, in view of large surface area of more than 113,000 km^2 for Indus at Kachura and substantial changes expected in the hydroclimatic trends upstream Shigar gauge, the discharge estimated by Mukhopadhyay and Khan (2014) seems to be a constant fraction of the Kachura discharge, rather than the derived Shigar discharge. On the other hand, instead of estimating post-1998 discharge at the Shigar gauge, we have derived the discharge for the Shigar-region, comprising Shigar sub-basin itself plus the adjacent region shown blank in the Figure 2. This was achieved by subtracting the mean discharge rates of all gauges upstream Shigar gauge from its immediate downstream Kachura gauge at each time step of every time scale analyzed. The procedure assumes that the gauges far from each other have negligible routing time delay at a mean monthly time scale and that such an approximation does not further influence the ascertained trends. Similar methodology has been adopted to derive discharge out of identified ungauged regions, such as, Karakoram, Himalaya, UIB-Central, UIB-West, UIB-West-lower and UIB-West-upper (Table 1).

We have considered the Karakoram region as the area of Hunza and Shyok sub-basins and Shigar-region, which are named as western, eastern and central Karakoram, respectively (Fig. 2). Similarly, we have considered drainage area of Indus at Kharmong as UIB-East while Shyok and Shigar-region together constitute UIB-Central. The rest of the UIB is considered as UIB-West (Fig. 2), which is further divided into upper and lower regions, keeping in view relatively large number of stations and distinct hydrological regimes. Such distinct regimes have been identified from the median hydrographs of each steam flow gauging station based on maximum runoff production timings. According to such division, UIB-West-lower and Gilgit are mainly snow-fed basins while Hunza is mainly glacier-fed basin (Fig. 3). Since most of the Gilgit basin area lies at Hindukush massifs, we call it Hindukush region. The combined area of lower part of UIB-West and UIB-east is mainly the northward slope of the Greater Himalaya, so we call this region as Himalaya.

We have analysed the field significance for those regions that contain at least two or more stations. To eliminate the effect of cross/spatial correlation amid station network on assessing the field significance of a particular region, Douglas et al. (2000) have proposed a bootstrap method. This method preserves the spatial correlation amid station network but eliminates its influence on testing the field significance based on MK statistics *S*. Similarly, Yue and Wang (2002) have proposed a regional average MK test in which they altered the variance of MK statistic by serial and cross correlations. Lately, Yue et al. (2003) proposed a variant of method proposed by Douglas et al. (2000), in which - instead of *S* - they considered counts of significant trends as representative variables for testing the field significance. This method favourably provides a measure of dominant field significant trend when local positive or negative significant trends are equal in number. Therefore, we have employed the method of Yue et al. (2003) for assessing the field significance. We have used a bootstrap approach (Efron, 1979) to resample the original network 1000 times in a way that the spatial correlation structure was preserved as described by Yue et al. (2003). We have counted both the number of local significant positive and number of significant negative trends, separately for each resampled network dataset using Eqn. 10:

$$C_f = \sum_{i=1}^{n} C_i \qquad (10)$$

Where n denotes total number of stations within a region and C_i denotes a count for statistically significant trend (at 90% level) at station, *i*. Then, we have obtained the empirical cumulative distributions C_f for both counts of significant positive and counts of significant negative trends, by ranking their corresponding 1000 values in an ascending order using Eqn.11:

$$P\left(C_f \leq C_f^r\right) = \frac{r}{N+1} \qquad (11)$$

Where r is the rank of C_f^r and N denotes the total number of resampled network datasets. We have estimated probability of the number of significant positive (negative) trends in actual network by comparing the number with C_f for counts of significant positive (negative) trends obtained from resampled networks (Eqn. 12).

$$P_{obs} = P\left(C_{f,obs} \leq C_f^r\right),\ where\ P_f = \begin{cases} P_{obs} & for\ P_{obs} \leq 0.5 \\ 1 - P_{obs} & for\ P_{obs} > 0.5 \end{cases} \qquad (12)$$

If expression, $P_f \leq 0.1$, is satisfied the trend over a region is considered to be field significant at the 90 % level.

The statistically assessed field significance of tendencies in meteorological variables is further validated against the physically-based evidence from the stream flow record. For this, we have compared the field significant climatic (mainly temperature) trend of a region with its stream flow trends (from installed and derived gauges). The qualitative agreement between the two can serve better in understanding the ongoing state of climatic changes over the UIB. Since most downstream gauge of Besham Qila integrates variability of all upstream gauges, it represents the dominant signal of change. Thus, an assessment of statistically based field significance was not required for the stream flow dataset.

We also assess the dependency of local hydroclimatic trends on their latitudinal, longitudinal and altitudinal distribution. We have intentionally avoided the interpolation of data and results in view of limitations of the interpolation techniques in a complex terrain of HKH region (Palazzi et al., 2013; Hasson et al., 2015a). Large offset of glaciological reports from the station based estimates of precipitation (Hasson et al., 2014b) further suggests that hydro-climatic patterns are highly variable in space and that the interpolation of data will further add to uncertainty, resulting in misleading conclusions.

5 Results

We present our trend analysis results for the 1995-2012 period in Tabular Figures 4-5 (and for the select time scales, in Fig. 4) while for the 1961-2012 period in Tabular Figure 6. The field significant trends in climatic variables and trends in discharge from the corresponding regions are presented in Tabular Figure 7.

5.1 Hydroclimatic trends

Mean maximum temperature

For Tx, we find that certain set of months exhibit a common response of cooling and warming within the annual course of time. Set of these months interestingly are different than those typically considered for seasons, such as, DJF, MAM, JJA, SON for winter, spring, summer and autumn, respectively (Fowler and Archer, 2005 and 2006; Khattak et al., 2011; Bocchiola and Diolaiuti, 2013). For the months of December, January, February and April, stations show a mixed response of cooling and warming tendencies by roughly equal numbers where cooling trend for Rattu in January, for Shendure in February and for Ramma in April are statistically significant (Tabular Fig. 4 and Fig. 8). Though no warming trend has been found to be statistically significant, all low altitude stations, except Gupis, exhibit a warming trend in the month of January. During months of March, May and November, most of the stations exhibit a warming trend, which is statistically significant at five stations (Gilgit, Yasin, Astore, Chillas and Gupis) and relatively higher in magnitude during March. Interestingly, warming tendencies during March are relatively higher in magnitude at low altitude stations as compared to high altitude stations. Most of the stations feature cooling tendencies during July-October (mainly the monsoon period). During such period, we find a statistically significant cooling at five stations (Dainyor, Shendure, Chillas, Gilgit and Skardu) in July, at two stations (Shendure and Gilgit) in August and at twelve stations (Hushe, Naltar, Ramma, Shendure, Ushkore, Yasin, Ziarat, Astore, Bunji, Chillas, Gilgit and Skardu) in September, while there is no significant cooling tendency in October (Tabular Fig. 4 and Fig. 8). Such cooling is almost similar in magnitude from low and high altitude stations and dominates during month of September followed by July because of higher magnitude and statistical significance agreed among large number of stations. Overall, we note that cooling trends dominate over the warming trends. On a typical seasonal scale, winter season generally shows a mixed behavior (cooling/warming) where only two stations (Dainyor and Rattu) suggest significant cooling. For the spring season, there is a high agreement for warming tendencies among the stations, which are significant only at Astore station. Again such warming tendencies during spring are relatively higher in magnitude than those at higher altitude stations. For summer and autumn, most of the stations feature cooling tendencies, which are significant for three stations (Ramma, Shendure and Shigar) in summer and for two stations (Gilgit and Skardu) in autumn. On annual time scale, high altitude stations within Astore basin (Ramma and Rattu) feature significant cooling trend.

While looking only at long term trends (Tabular Fig. 6), we note that summer cooling (warming outside summer) in Tx is less (more) prominent and insignificant (significant) at stations of relatively high (low) elevation, such as, Skardu, Gupis, Gilgit and Astore (Bunji and Chillas). The absence of a strong long-term winter warming contrasts with what found for the shorter period 1995-2012. In fact, strong warming is restricted to spring season mainly during March and May months. Similarly, long-term summer cooling period of June-October has been shortened to July-October.

Mean minimum temperature

The dominant feature of Tn is the robust winter warming in Tn during November-June, which is found for most of the stations (Tabular Fig. 4 and Fig. 8). Contrary to warming in Tx, warming trend in Tn is higher in magnitude among the high altitude stations than among the low altitude stations. During the period of July-October, we found a significant cooling of Tn at four stations (Gilgit, Naltar, Shendure and Ziarat) in July, at eight stations (Hushe, Naltar, Ushkore, Yasin, Ziarat, Astore, Chillas and Gilgit) in September and only at Skardu in October. In August, stations show warming tendencies, which are relatively small in magnitude and only significant at Gilgit station. Similar to Tx, cooling in Tn during July-October dominates during the month of September suggesting a relatively higher magnitude and larger number of significant trends (Fig. 8). Also, such cooling features more or less similar magnitude of a trend among high and low altitude stations as for Tx. Similarly, cooling trends in Tn mostly dominate over the warming trends as in case of Tx. On a typical seasonal scale, winter and spring seasons feature warming trends, while summer season exhibit cooling trend and there is a mixed response for the autumn season. Warming trend dominates during the spring season. Here, we emphasize that a clear signal of significant cooling in September has been lost while averaging it into October and November months for autumn season. This is further notable from the annual time scale, on which a warming trend is generally dominated that is statistically significant at five stations (Deosai, Khunjrab, Yasin, Ziarat and Gilgit). The only significant cooling trend on annual time scale is observed at Skardu station.

While looking only at low altitude stations (Tabular Fig. 6), we note that long term non-summer warming (summer cooling) in Tn is less (more) prominent and insignificant (significant) at stations of relatively high (low) elevation, such as, Skardu, Gupis, Gilgit and Astore (Bunji and Chillas).

Mean temperature

Trends in Tavg are dominated by trends in Tx during July-October while these are dominated by Tn, during the rest of year (Tabular Figs. 4-5). Similar to Tx, the Tavg features a significant cooling in July at four stations (Dainyor, Naltar, Chillas and Skardu), in September at ten stations (Hushe, Naltar, Rama, Shendure, Ushkore, Yasin, Ziarat, Astore, Chillas and Skardu) and in October only at Skardu station (Tabular Fig. 5 and Fig. 8). In contrast, we have observed a significant warming at Ziarat station in February, at five stations (Deosai, Dainyor, Yasin, Astore and Gupis) in March and at three stations (Khunjrab, Gilgit and Skardu) in November. However, the trend analysis on typical seasonal averages suggests warming of winter and spring seasons, which is higher in magnitude as compared to the observed cooling in summer and autumn seasons. This specific fact has led to a dominant warming trend by most of the station at annual time scale, which is higher in magnitude at high altitude stations, mainly due to their dominated winter warming as compared to low altitude stations (Shrestha et al., 1999; Liu and Chen, 2000).

The long term trends generally suggest cooling tendencies during the July-October while warming for the rest of year. On seasonal scale, low altitude stations unanimously exhibit summer cooling over the long term record, which is mostly significant. A mixed response is shown for other time scales.

Diurnal temperature range

For the DTR, most of the stations show its drop throughout a year except during months of March and May, where particularly low altitude stations show its increase mainly due to higher warming in Tx than in Tn or higher cooling in Tn than in Tx (Tabular Fig. 4 and Fig. 8). Two stations (Chillas and Skardu) show a significant widening of DTR in May, followed by Chillas station in March, Deosai in August and Gupis in October months. Conversely, we observe high inter-station agreement of significant DTR decrease in September followed by in February. Such a trend is associated with the higher magnitude of cooling in Tx than in Tn (e.g. in September), cooling in Tx but warming in Tn or higher warming in Tn than in Tx (e.g. in February). We note that long term trends of increasing DTR throughout a year from low altitude stations (Tabular Fig. 6) are now mainly restricted to the period March-May, and within the months of October and December over the period 1995-2012. Within the rest of year, DTR has been decreasing since last two decades. Overall, high altitude stations exhibit though less strong but a robust pattern of year round significant decrease in DTR as compared to low altitude stations.

Total precipitation

We find that most of the stations show a clear signal of dryness during the period March-June, which is either relatively higher or similar at high altitude station than at low altitude stations (Table 5 and Fig. 4). During such period, significant drying is revealed by seven stations (Deosai, Dainyor, Yasin, Astore, Chillas, Gupis and Khunjrab) in March, by five stations (Dainyor, Rattu, Astore, Bunji and Chillas) in April, by two stations (Dainyor and Rattu) in May and by four stations (Dainyor, Rama, Rattu and Shigar) in June. We have observed similar significant drying during August by three stations (Rattu, Shigar and Gupis) and during October by three stations (Rattu, Shendure and Yasin). The Rattu station features a consistent drying trend throughout a year except during the months of January and February where basically a neutral behavior is observed. Stations feature high agreement for an increasing trend during winter season (December to February) and during the month of September, where such increase is higher in magnitude at high altitude stations as compared to low altitude stations. We note that most of the stations within the UIB-West-upper region (monsoon dominated region) exhibit an increasing trend. Shendure, Yasin, Ziarat, Rattu, Shigar and Chillas are stations featuring significant increasing trend in either all or at least in one of the monsoon months. Such precise response of increasing or decreasing trend at monthly scale is averaged out on a seasonal time scale, on which autumn and winter seasons show an increase while spring and summer seasons show a decrease. Annual trends in precipitation show a mixed response by roughly equal number of stations.

From our comparison of medium term trends at low altitude stations with their long term trends (See Table 5 and 6), we note that trends over the recent decades exhibit much higher magnitude of dryness during spring months, particularly for March and April, and of wetness particularly within the month of September – the last monsoonal month. Interestingly, shifts in the trends have been noticed during the summer months (June-August) where trends over recent decades exhibit drying but the long-term trends suggest wetter conditions. Only increase in September precipitation is consistent between the long-term trend and trend obtained over 1995-2012 at low altitude stations.

Discharge

Based on the median hydrograph of each stream flow gauge for the UIB (Fig. 3), we clearly show that both snow and glacier fed/melt regimes can be differentiated based on their runoff production time. Figure 3 suggests that Indus at Kharmong (Eastern UIB), Gilgit at Gilgit (Hindukush) and Astore at Doyian are primarily snow fed basins, generally featuring their peak runoff in July. The rest of the basins are mainly glacier fed basins that feature their peak runoff in August.

Based on 1995-2012 period, our trend analysis suggests an increasing trend from most of the hydrometric stations during October-June, with highest magnitudes in May-June (Tabular Fig. 5). A discharge increase pattern seems to be more consistent with tendencies in the temperature record than in precipitation record. In contrast, most of the hydrometric stations experience a decreasing trend of discharge during the month of July, which is statistically significant out of five (Karakoram, Shigar, Shyok, UIB-Central and Indus at Kachura) regions, owing to drop in July temperatures. These regions, showing significant drop in discharge, are mainly high-altitude/latitude glacier-fed regions within the UIB. For August and September months, there is a mixed response, however, statistically significant trends suggest an increase in discharge out of two (Hindukush and UIB-West-lower) regions in August and out of four (Hindukush, western-Karakoram, UIB-West-lower and UIB-west) regions during September. We note that despite of the dominant cooling during September, discharge mainly drops during July, suggesting a strong impact of the cooling during such a month. Discharge from the whole UIB also decreases during the month of July, however, such a drop is not statistically significant. Possibly, the lack of statistical significance in the UIB discharge trend may have been caused by the integrated response from sub-regions, and that significant signal might appear when looking at higher temporal resolution data, such as 10-day or 5-day averages. During winter, spring and autumn seasons, discharge at most sites feature increasing trend while during summer season and on an annual time scale there is a mixed response.

Our long-term analysis reveals a positive trend of stream flow during the period (November to May) from most of the sites/regions (Tabular Fig. 6). Such a positive trend is particularly higher in magnitude in May and also significant at relatively large number of gauging sites (14 among 16). In contrast to November-May period, there is a mixed signal of rising and falling stream flow trend among sites during June-October. The increasing and decreasing stream flow trends at monthly time scale exhibit similar response when aggregated on a typical seasonal or annual time scales. Winter discharge features an increasing trend while for the rest of seasons and on an annual time scale, sites mostly exhibit a mixed response.

While comparing the long-term trends with the trends assessed from recent two decades, we note most prominent shifts in the sign of trends during the seasonal transitional month of June and within the high flow months July-September. This may attribute to higher summer cooling together with the enhanced precipitation under the influence of monsoonal precipitation regime in recent decades. For instance, long term trend suggests that discharge out of eastern-, central- and whole Karakoram, UIB-Central, Indus at Kachura, Indus at Partab Bridge and Astore regions is increasing while rest of regions feature a decreasing trend. However, trend from the recent two decades suggests the opposite sign of discharge coming out of such regions, except the regions of Astore, Hindukush, UIB-West-upper and its sub-regions, which consistently show similar sign of change.

5.2 Field significance and physical attribution

Based on number of local significant trends, we analyze their field significance for both positive and negative trends, separately (Tabular Fig. 7). We present mean slope of the field significant trends in order to present the dominant signal from the region. Our results show a unanimous field significant warming for most of the regions in March followed by in August. Similarly, we generally find a field significant decreasing trend in March precipitation over all regions, except Karakoram and UIB-Central regions. We find a field significant cooling over all regions during the months of July, September and October, which on a seasonal scale, dominates during autumn season followed by summer season. Interestingly, we note that most of the climatic trends are not field-significant during the transitional (or pre-monsoon) period of April-June. We found a general trend of narrowing DTR, which is associated with either warming of Tn against cooling of Tx or relatively lower cooling in Tn than in Tx. Field significant drying of the lower latitudinal regions (Astore, Himalaya, UIB-West-lower - generally snow-fed regions) is also observed particularly during the period March-September, thus for the spring and summer and for the annual time scale. On the other hand, we found an increasing (decreasing) trend in precipitation during winter and autumn (spring and summer) seasons for the Hindukush, UIB-West, UIB-West-upper and whole UIB while for the western Karakoram such increase in precipitation is observed during winter season only. For the whole Karakoram and UIB-central regions, field significant increasing trend in precipitation is observed throughout a year except during the spring season where no signal is evident.

We have noted that for most of the regions the field significant cooling and warming trends are in good agreement against the trends in discharge from the corresponding regions. Such an agreement is high for summer months, particularly for July, and during winter season, for the month of March. Few exceptions to such consistency are the regions of Himalaya, UIB-West and UIB-West-lower, for which, in spite of the field significant cooling in July, discharge still features a positive trend. However, we note that the magnitude of the increase in July discharge has substantially dropped when compared to increases in previous (June) and following (August) months. Such a substantial drop in July discharge increase rate is again consistent with the prevailing field significant cooling during July for the UIB-West and UIB-West-lower regions. Thus, the identified field significant climatic signals for the considered regions are further confirmed by their observed discharge tendencies.

Interestingly, we note that generally magnitude of cooling during September dominates the magnitude of cooling during July while magnitude of warming during March dominates the magnitude of warming during May. However, subsequent runoff response from the considered regions does not correspond with the magnitude of cooling and warming trends. In fact, most prominent increase in discharge is observed in May while decrease in July, suggesting them months of effective warming and cooling, respectively. Generally, periods of runoff decrease (in a sequence) span from May to September for the Karakoram, June to September for the UIB-Central, July to August for the western-Karakoram and UIB-West-upper, July to November for the Astore and only over July for the Hindukush and UIB regions. Regions of UIB-West-lower and Himalaya suggest decrease in discharge during months of April and February, respectively.

5.3 Tendencies versus latitude, longitude and altitude

In order to explore the geographical dependence of the climatic tendencies, we plot tendencies from the individual stations against their longitudinal, latitudinal and altitudinal coordinates (Figs. 9-11). We note that summer cooling is observed in all stations; however the stations between 75-76^{o} E additionally show cooling during the month of May in Tx, Tn and Tavg. Within 74-75^{o} E, stations generally show a positive gradient towards west in terms of warming and cooling, particularly for Tn. DTR generally features a narrowing trend where magnitude of such a trend tends to be higher west of 75^{o} longitude (Astore basin). Precipitation generally increases slightly but decreases substantially at 75^{o} longitude. Discharge decreases at highest (UIB-east) and lowest (UIB-west) gauges in downstream order, while increases elsewhere.

Cooling or warming trends are prominent at higher latitudinal stations, particularly for cooling in Tx and warming in Tn. Highest cooling and warming in Tavg is noted around 36^{o}N. Similarly, we have observed a highest cooling in Tx and warming in Tn, while Tx cooling dominates in magnitude as evident from Tavg. DTR generally tends to decrease towards higher latitudes where magnitude of decrease in a particular season/month is larger than increase in it for any other season/month. Highest increasing or decreasing trend in precipitation is observed below 36^{o}N. Whereas station below 35.5^{o}N show substantial decrease in annual precipitation mainly due to decrease in spring season. The stations between 35.5-36^{o}N show increase in annual precipitation mainly due to increase in winter precipitation.

The magnitude of cooling (warming) in Tn decreases (increases) at higher elevations. Stations below 3500 m asl feature relatively higher magnitude of cooling in Tx, which is also higher than warming trends in Tx as well as in Tn. Such signals are clear from tendencies in Tavg. The low-altitude stations and the stations at highest elevation show the opposite response, featuring a pronounced warming in Tavg than its cooling in respective months/seasons. We note that precipitation trends from higher altitude stations are far more pronounced than in low altitude station, and clearly suggest drying of spring but wetting of winter seasons. Tendencies in DTR in high altitude stations are consistent qualitatively and quantitatively as compared to tendencies in low altitude stations.

6 Discussions

Cooling trends

Our long term updated analysis suggests that summer and autumn cooling trends are mostly consistent with previously reported trends (Fowler and Archer, 2005 and 2006; Khattak et al., 2011), and with reports of increasing summer snow cover extent over the UIB (Hasson et al., 2014b). The overall warming over Pakistan (and UIB) reported by Río et al. (2013) is however in direct contrast to the cooling tendencies reported here and by the above mentioned studies, regardless of the seasons. Our findings of long term cooling trends during the monsoon period are also in high agreement with reports of Sheikh et al. (2009) for the study region, which is consistently reported for the neighboring regions, such as, Nepal, Himalayas (Sharma et al., 2000; Cook et al., 2003), northwest India (Kumar et al., 1994), Tibetan Plateau (Liu and Chen, 2000), central China (Hu et al., 2003), and central Asia (Briffa et al., 2001) for the investigated periods.

More importantly, the station-based cooling trends are found field significant for all identified sub-regions of the UIB mostly in July, September and October, coinciding with the months of monsoonal onset and retreat, and also with the glacier melt season. Thus, field significant cooling is further depicted from the trends in discharge out of respective regions, specifically during July, when discharge either exhibit falling or weaker rising trends relative to contiguous months due to declining glacial melt. The field significant cooling and subsequent discharge behaviour is attributed to the incursions of south Asian summer monsoonal system and its precipitation (Cook et al., 2003) into the Karakoram, through crossing Himalayas, and into the UIB-West region, for which Himalayan barrier does not exist. Such phenomenon seems to be accelerated at present under the observed increasing trend in cloud cover, in number of wet days - particularly over the UIB-West region (Bocchiola and Diolaiuti, 2013) - and subsequently in total amount of precipitation during the monsoon season. The enhanced monsoonal influence in the far north-west over the UIB-West region, and within the Karakoram, is consistent with the extension of the monsoonal domain northward and westward under the global warming scenario as projected by the multi-model mean from climate models participating in the Climate Model Intercomparison Project Phase 5 (CMIP5 - Hasson et al., 2015a). Such hypothesis further needs a detailed investigation and it is beyond the scope of present study. Nevertheless, increasing cloud cover due to enhanced influence and frequent incursions of the monsoonal system leads to reduction of incident downward radiations and results in cooling (or less warming) of Tx. Forsythe et al. (2015) have consistently observed influence of the cloud radiative effect on the near surface air temperature over the UIB. The enhanced cloudy conditions most probably are mainly responsible for initially higher warming in Tn through longwave cloud radiative effect. Given that such cloudy conditions persist longer in time, Tx and Tn are more likely tend to cool. Under the clear sky conditions, cooling in Tx further continues as a result of evaporative cooling of the moisture-surplus surface under precipitation event (Wang et al., 2014) or due to irrigation (Kueppers et al., 2007). Han and Yang (2013) found irrigation expansion over Xinjiang, China as a major cause of observed cooling in Tavg, Tx and Tn during May-September over the period 1959-2006. Further, higher Tn drop observed over UIB-West-lower region during winter months can be attributed to intense night time cooling of the deforested, thus moisture deficit, bare soil surface, exposed to direct day time solar heating as explained by Yadav et al. (2004).

Due to cooling trends, the UIB though features some responses consistent with the neighboring region and as observed worldwide but reason for such common responses may still be contradictory. For instance, field significant decreasing trend in DTR during July-October period is attributed to stronger cooling in Tx than in Tn, which is contrary to the reason of decreasing DTR observed worldwide and over the northeast China (Jones et al., 1999; Wang et al., 2014).

Warming trends

Long term warming during November-May is generally found consistent with previously reported warming trends (Fowler and Archer, 2005 and 2006; Sheikh et al., 2009; Khattak et al., 2011; Río et al., 2013) as well as with decreasing snow cover extent during spring (1967-2012) in the Northern Hemisphere and worldwide (IPCC, 2013) and during winter (2001-2012) over the study region (Hasson et al., 2014b). However, warming generally dominates in spring months, consistent with findings of Sheikh et al. (2009) and Río et al. (2013). Being consistent with recent acceleration of global climatic changes (IPCC, 2013), such spring warming is observed higher over the 1995-2012 period, particularly in March and May, respectively. Further, warming in Tx (Tn) is more pronounced at low (high) altitude stations. More importantly, the station-based spring warming is found field significant in March over almost all identified sub-regions of the UIB. Under the drying spring scenario, less cloudy conditions associated with increasing number of dry days for the westerly precipitation regime (Hasson et al., 2015a) together with snow-albedo feedback can partly explain such warming during spring months.

Contrary to spring warming, our analysis suggests generally a field significant cooling in winter, which is in direct contrast to long term warming trends analyzed here and those previously reported (Fowler and Archer, 2005 and 2006; Sheikh et al., 2009; Khattak et al., 2011). Such a recent shift of winter warming to cooling is consistently observed over eastern United States, southern Canada and much of the northern Eurasia (Cohen et al., 2012). The recent winter cooling is a result of falling tendency of winter time Arctic Oscillation, which partly driven dynamically by the anomalous increase in autumnal Eurasian snow cover (Cohen and Entekhabi, 1999), can solely explain largely the weakening (strengthening) of the westerlies (maridional flow) and favors anomalously cold winter temperatures and their falling trends (Thompson and Wallace, 1998 and 2001; Cohen et al., 2012). Weakening of the westerlies during winter may explain an aspect of well agreed drying during subsequent spring season, and may further be related to more favorable conditions for the southerly monsoonal incursions into the UIB.

Wetting and drying trends

Enhanced influence of the late-monsoonal precipitation increase at high altitude stations suggests field significant increasing trend in precipitation for the regions at relatively higher latitudes, such as, Hindukush and UIB-Central, and thus, for the UIB-West-upper, Karakoram and the whole UIB. This is in good agreement with the projected intensification of south

Asian summer monsoonal precipitation regime under enhanced greenhouse gas emission scenarios (Hasson et al., 2013, 2014a & 2015a). At the low altitude stations, shifts of the long-term trends of increasing summer precipitation (June-August) to drying over the period 1995-2012 indicate a transition towards weaker monsoonal influence at lower levels. This may attribute to multi-decadal variability that is associated with the global indices, such as, NAO and ENSO, influencing the distribution of large scale precipitation over the region (Shaman and Tziperman, 2005; Syed et al., 2006).

The field significant trends of precipitation increase during winter but decrease during spring season is associated with certain changes in the westerly precipitation regime under changing climate. For instance, field significant drying in spring (except for Karakoram) is mainly consistent with the weakening and northward shift of the mid-latitude storm track (Bengtsson et al., 2006) and increase in the number of dry days within spring season for the westerly precipitation regime (Hasson et al., 2015a). On the other hand, observed increase in the winter precipitation for relatively high latitudinal regions is consistent with the observations as well as with the future projections of more frequent incursions of the westerly disturbances into the region (Ridley et al., 2013; Cannon et al., 2015; Madhura et al., 2015). In view of more frequent incursions of the monsoonal system and westerly disturbances expected in the future and certain changes projected for the overall seasonality/intermittency of their precipitation regimes by the climate models (Hasson et al., 2015a), significant changes in the timings of melt water availability from the UIB are speculated. Such hypothesis can be tested by assessing changes in the seasonality of precipitation and runoff based on observations analyzed here and also through modelling melt water runoff from the region under prevailing climatic conditions.

Water availability

The long term discharge tendencies are consistent with earlier reports from Khattak et al. (2011) for Indus at Kachura, and UIB regions and from Farhan et al. (2014) for Astore. Similarly, rising and falling discharge trends from Shyok and Hunza sub-basins, respectively, are consistent with Mukhopadhyay et al. (2015). The discharge trends from Shigar-region, though statistically insignificant, are only partially consistent with Mukhopadhyay and Khan (2014), exhibiting agreement for an increasing trend in June and August but a decreasing trend in July and September.

We note prominent shifts of the long term trends of rising melt-season discharge into falling over the period 1995-2012 for mostly the glacier-fed regions (Indus at Kachura, Indus at Partab Bridge, Eastern-, Central- and whole-Karakoram and UIB-Central). Such shifts may attribute to higher summer cooling together with certain changes in the precipitation regime. Change in sign of discharge trend for eastern-Karakoram (Shyok) is expected to substantially alter discharge at Kachura site, thus deriving a Shigar discharge by applying previously identified constant monthly fractions to the downstream Kachura gauge (Mukhopadhyay and Khan, 2014) would less likely yield a valid Shigar discharge for its period of missing record (1999-2010). Some regions, such as, UIB-West-upper and its sub-regions together with Astore and whole UIB are the regions consistently showing same sign of change in their long term trend when compared to the trends derived over the period 1995-2012.

Over the 1995-2012 period, decreasing stream flow trend observed for mainly the glacier-fed regions is mostly significant in July. Though cooling in July is less prominent than cooling in September, it is much effective as it coincides with the main glacial melt season. Such drop in July discharge, owing to decreased melting, results in reduced melt water availability, but at the same time, indicates positive basin storage, in view of enhanced moisture input. Similarly, increase in discharge during May and June is due to the observed warming, which though less prominent than warming in March, is much effective since it coincides with the snow melt season. This suggests an early melt of snow and subsequent increase in the melt water availability, but concurrently, a lesser amount of snow available for the subsequent melt season. Such distinct changes in snow melt and glacier melt regimes are mainly due to the non-uniform climatic changes on a sub-seasonal scale. This further emphasizes on a separate assessment of changes in both snow and glacier melt regimes, for which an adequate choice is the hydrological models that are able to distinctly simulate snow and glacier melt processes. Nevertheless, changes in both snow and glacier melt regimes all together can result in a sophisticated alteration of the hydrological regimes of the UIB, requiring certain change in the operating curve of the Tarbela reservoir in future.

The discharge change pattern seems to be more consistent with field significant temperature trends than with precipitation trends. This points to the fact that the cryosphere melting processes are the dominating factor in determining the variability of the rivers discharge in the study region. However, changes in precipitation regime can still influence substantially the melt processes and subsequent meltwater availability. For instance, monsoon offshoots intruding into the region ironically result in declining river discharge (Archer, 2004), since crossing the Himalaya such monsoonal incursions mainly drop moisture over the high altitude regions and in the form of snow (Wake, 1989; Böhner, 2006). In that case, fresh snow and clouds firstly reduce the incident energy due to high albedo that results in immediate drop in the melt. Secondly, fresh snow insulates the underlying glacier/ice, slowing down the whole melt process till earlier albedo rates are achieved. Thus, melting of snow and glaciers and subsequent overall meltwater availability is inversely correlated to the number of snowfall events/days during the melt season (Wendler and Weller, 1974; Ohlendorf et al., 1997).

In view of the sparse network of meteorological observations analyzed here, we need to clarify that the observed cooling and warming is only an aspect of the wide spread changes prevailing over the wide-extent UIB basin. This is much relevant for the UIB-Central region where we have only one station each from the eastern- and central- Karakoram (UIB-Central), not exclusively representative of their hydro-climatic state. Thus, field significant results for the whole Karakoram region are mainly dominated by contribution of relatively large number of stations within the western-Karakoram. Nevertheless, glaciological studies, reporting and supporting the Karakoram anomaly (Hewitt, 2005; Scherler et al., 2011; Bhambri et al., 2013) and possibly a non-negative mass balance of the aboded glaciers within eastern- and central-Karakoram (Gardelle et al., 2013 - contrary at shorter period – Kääb et al., 2015), further reinforce our findings. Moreover, our results agree remarkably well with the local narratives of climate change as reported by Gioli et al. (2013). In view of such consistent findings, we are confident that the observed signal of hydroclimatic changes dominates at present, at least qualitatively. Furthermore, climatic change signal observed within the mountainous environments can vary with respect to altitude (MRI, 2015; Hasson et al., 2015b). Such elevation dependent signal of climatic change is somewhat depicted by the sparse observations analysed here. However, the robust assessment of such an aspect requires spatially complete observational database.

The hydro-climatic regime of the UIB is substantially controlled by the interaction of large scale circulation modes and their associated precipitation regimes, which are in turn controlled by the global indices, such as, NAO and ENSO etc. The time period covered by our presented analysis is not long enough to disintegrate such natural variability signals from the transient climate change. Such phenomena need to be better investigated based upon longer period of observational record for in depth understanding of the present variability in the hydrological regime of the UIB and for forecasting future changes in it. For future projections, global climate models at a broader scale and their downscaled experiments at regional to sub-regional scales are most vital datasets available, so far. However, a reliable future change assessment over the UIB from these climate models will largely depend upon their satisfactory representation of the prevailing climatic patterns and explanation of their teleconnections with the global indices, which are yet to be (fully) explored. The recent generations of the global climate models (CMIP5) feature various systematic biases (Hasson et al., 2013, 2014a and 2015a) and exhibit diverse skill in adequately simulating prevailing climatic regimes over the region (Palazzi et al., 2014; Hasson et al., 2015a). We deduce that realism of these climate models about the observed winter cooling over the UIB much depends upon reasonable explanation of autumnal Eurasian snow cover variability and its linkages with the large scale circulations (Cohen et al., 2012). On the other hand, their ability to reproduce summer cooling signal is mainly restricted by substantial underestimation of the real extent of the south Asian summer monsoon owing to underrepresentation of High-Asian topographic features and absence of irrigation waters (Hasson et al., 2015a). However, it is worth investigating data from high resolution Coordinated Downscaled Experiments (CORDEX) for South Asia for representation of the observed thermal and moisture regimes over the study region and whether such dynamically fine scale simulations feature an added value in their realism as compared to their forced CMIP5 models. Given these models do not adequately represent the summer and winter cooling and spring warming phenomena, we argue that modelling melt runoff under the future climate change scenarios as projected by these climate models is still not relevant for the UIB as stated by Hasson et al. (2014b). Moreover, it is not evident when the summer cooling phenomenon will end. Therefore, we encourage the impact assessment communities to model the melt runoff processes from the UIB, taking into account more broader spectrum of future climate change uncertainty, thus under both prevailing climatic regime as observed here and as projected by the climate models, relevant for short and long term future water availability, respectively.

7 Conclusions

Our findings supplement the ongoing research on addressing the question of water resources dynamics in the region, such as, ‘Karakoram Anomaly’ and the future water availability. In view of recently observed shifts and acceleration of the hydroclimatic trends over HKH ranges within the UIB, we speculate an enhanced influence of the monsoonal system and its precipitation regime during the late-melt season. On the other hand, changes in the westerly disturbances and in the associated precipitation regime are expected to drive changes observed during winter, spring and early-melt season. The observed hydroclimatic trends, suggesting distinct changes within the period of mainly snow and glacier melt, indicate at present strengthening of the nival while suppression of the glacial melt regime, which all together will substantially alter the hydrology of the UIB. However, such aspects need to be further investigated in detail by use of hydrological modelling, updated observational record and suitable proxy datasets. Nevertheless, changes presented in the study earn vital importance when we consider the socio-economic effects of the environmental pressures. The melt water reduction will result in limited water availability for the agricultural and power production downstream and may results in a shift in solo-season cropping pattern upstream. This emphasizes the necessary revision of WAPDA's near future plan i.e. Water Vision 2025 and recently released first climate change policy by the Government of Pakistan, in order to address adequate water resources management and future planning in relevant direction.

Acknowledgement: The authors acknowledge Water and Power Development Authority (WAPDA), Pakistan and Pakistan Meteorological Department (PMD) for providing the hydroclimatic data. S. Hasson and J. Böhner acknowledge the support of BMBF, Germany's Bundle Project CLASH/Climate variability and landscape dynamics in Southeast-Tibet and the eastern Himalaya during the Late Holocene reconstructed from tree rings, soils and climate modeling. Authors also acknowledge the support from CliSAP/Cluster of excellence in the Integrated Climate System Analysis and Prediction.

References

Ahmad, Z., Hafeez, M., Ahmad, I.: Hydrology of mountainous areas in the upper Indus Basin, Northern Pakistan with the perspective of climate change, Environmental Monitoring and Assessment, 184, 9, pp 5255-5274, 2012.

Alford, D.: Hydrology and Glaciers in the Upper Indus Basin. Department of Geography, University of Montana, Billings, Montana, USA. 2011.

Ali, G., Hasson, S., and Khan, A. M.: Climate Change: Implications and Adaptation of Water Resources in Pakistan, GCISC-RR-13, Global Change Impact Studies Centre (GCISC), Islamabad, Pakistan, 2009.

Archer, D. R. and Fowler, H. J.: Spatial and temporal variations in precipitation in the Upper Indus Basin, global teleconnections and hydrological implications, Hydrol. Earth Syst. Sci., 8, 47–61, doi:10.5194/hess-8-47-2004, 2004.

Archer, D. R.: Contrasting hydrological regimes in the upper Indus Basin, J. Hydrol., 274, 19–210, 2003.

Archer, D. R.: Hydrological implications of spatial and altitudinal variation in temperature in the Upper Indus Basin. Nord. Hydrol, 35 (3), 209–222, 2004.

Arendt, A., A. Bliss, T. Bolch, J.G. Cogley, A.S. Gardner, J.-O. Hagen, R. Hock, M. Huss, G. Kaser, C. Kienholz, W.T. Pfeffer, G. Moholdt, F. Paul, V. Radić, L. Andreassen, S. Bajracharya, N.E. Barrand, M. Beedle, E. Berthier, R. Bhambri, I. Brown, E. Burgess, D. Burgess, F. Cawkwell, T. Chinn, L. Copland, B. Davies, H. De Angelis, E. Dolgova, L. Earl, K. Filbert, R. Forester, A.G. Fountain, H. Frey, B. Giffen, N. Glasser, W.Q. Guo, S. Gurney, W. Hagg, D. Hall, U.K. Haritashya, G. Hartmann, C. Helm, S. Herreid, I. Howat, G. Kapustin, T. Khromova, M. König, J. Kohler, D. Kriegel, S. Kutuzov, I. Lavrentiev, R. LeBris, S.Y. Liu, J. Lund, W. Manley, R. Marti, C. Mayer, E.S. Miles, X. Li, B. Menounos, A. Mercer, N. Mölg, P. Mool, G. Nosenko, A. Negrete, T. Nuimura, C. Nuth, R. Pettersson, A. Racoviteanu, R. Ranzi, P. Rastner, F. Rau, B. Raup, J. Rich, H. Rott, A. Sakai, C. Schneider, Y. Seliverstov, M. Sharp, O. Sigurðsson, C. Stokes, R.G. Way, R. Wheate, S. Winsvold, G. Wolken, F. Wyatt, N. Zheltyhina, 2015, Randolph Glacier Inventory – A Dataset of Global Glacier Outlines: Version 5.0. Global Land Ice Measurements from Space, Boulder Colorado, USA. Digital Media. 2015.

Batura Investigations Group: The Batura Glacier in the Karakoram Mountains and its variations, Scientia Sinica, 22, 958–974, 1979.

Bengtsson, L., Hodges, I. K., and Roeckner, E.: Storm tracks and climate change, J. Climate, 19, 3518–3542, 2006.

Bhambri, R., Bolch, T., Kawishwar, P., Dobhal, D. P., Srivastava, D., and Pratap, B.: Heterogeneity in glacier response in the upper Shyok valley, northeast Karakoram, The Cryosphere, 7, 1385-1398, doi:10.5194/tc-7-1385-2013, 2013.

Bocchiola, D., and Diolaiuti, G.: Recent (1980–2009) evidence of climate change in the upper Karakoram, Pakistan, Theor Appl Climatol, 113:611–641, 2013.

Böhner, J.: General climatic controls and topoclimatic variations in Central and High Asia, Boreas, 35, 279–295, 2006.

Bookhagen, B. and Burbank, D.W.: Toward a complete Himalayan hydrological budget: spatiotemporal distribution of snowmelt and rainfall and their impact on river discharge, J. Geophys. Res., 115, p. F03019, 2010.

Briffa, K. R., T. J. Osborn, F. H. Schweingruber, I. C. Harris, P. D. Jones, S. G. Shiyatov, and E. A. Vaganov,: Low frequency temperature variations from northern tree ring density network. J. Geophys. Res., 106, 2929–2941, 2001.

Brown, E.T., R. Bendick, D.L. Bourlès, V. Gaur, P. Molnar, G.M. Raisbeck, F. Yiou Early Holocene climate recorded in geomorphological features in Western Tibet Palaeogeogr. Palaeoclimatol. Palaeoecol., 199 (1–2) (2003), pp. 141–151 http://dx.doi.org/10.1016/S0031-0182(03)00501-7

Cannon, F., Carvalho, L. M. V., Jones, C., and Bookhagen, B.: Multi-annual variations in winter westerly disturbance activity affecting the Himalaya, Clim Dyn, 44:441–455, 2015. DOI 10.1007/s00382-014-2248-8

Cohen J and Entekhabi D.: Eurasian snow cover variability and Northern Hemisphere climate predictability Geophys. Res. Lett. 26 345–8, 1999.

Cohen, J. L., Furtado, J. C., Barlow, M. A., Alexeev V. A., and Cherry, J. E.: Arctic warming, increasing snow cover and widespread boreal winter cooling, Environ. Res. Lett. 7 014007 (8pp), 2012.

Conrad, V. and Pollak, C.: Methods in Climatology, Harvard University Press, Cambridge, MA, 459 pp, 1950.

Cook, E. R., Krusic, P. J. and Jones, P. D.: Dendroclimatic signals in long tree-ring chronologies from the Himalayas of Nepal. Int. J. Climatol., 23, 707–732, 2003.

Douglas EM, Vogel RM, Kroll CN. Trends in floods and low flows in the United States: impact of spatial correlation. Journal of Hydrology 240: 90–105, 2000.

Efron, B., Bootstrap methods: another look at the jackknife. Ann. Stat. 7 (1), 1-26, 1979.

Falvey, M., Garreaud, R.D., Regional cooling in a warming world: Recent temperature trends in the southeast Pacific and along the west coast of subtropical South America (1979–2006). Journal of Geophysical Research, 114, (D04102), 1–5, 2009.

Farhan, S. B., Zhang, Y., Ma, Y., Guo, Y. and Ma, N.: Hydrological regimes under the conjunction of westerly and monsoon climates: a case investigation in the Astore Basin, Northwestern Himalaya, Climate Dynamics, DOI: 10.1007/s00382-014-2409-9, 2014.

Forsythe, N., Fowler, H.J., Blenkinsop, S., Burton, A., Kilsby, C.G., Archer, D.R., Harpham, C., Hashmi., M. Z.: Application of a stochastic weather generator to assess climate change impacts in a semi-arid climate: The Upper Indus Basin, Journal of Hydrology, 517, 1019–1034, 2014.

Forsythe, N., Hardy, A. J., Fowler, H. J., Blenkinsop, S., Kilsby, C. G., Archer, D. R., and Hashmi, M. Z.: A Detailed Cloud Fraction Climatology of the Upper Indus Basin and Its Implications for Near-Surface Air Temperature. J. Climate, 28, 3537–3556, 2015.

Fowler, H. J. and Archer, D. R.: Conflicting Signals of Climatic Change in the Upper Indus Basin, J. Climate, 9, 4276–4293, 2006.

Fowler, H. J. and Archer, D. R.: Hydro-climatological variability in the Upper Indus Basin and implications for water resources, Regional Hydrological Impacts of Climatic Change – Impact Assessment and Decision Making (Proceedings of symposium S6, Seventh IAHS Scientific Assembly at Foz do Iguaçu, Brazil, IAHS Publ., 295, 2005.

Gardelle, J., Berthier, E., Arnaud, Y., and Kääb, A.: Region–wide glacier mass balances over the Pamir-Karakoram-Himalaya during 1999–2011, The Cryosphere, 7, 1263–1286, doi:10.5194/tc-7-1263-2013, 2013.

Gioli, G., Khan, T., and Scheffran, J.: Climatic and environmental change in the Karakoram: making sense of community perceptions and adaptation strategies. Regional Environmental Change, 14, 1151-1162, 2013

Han, S., and Yang, Z.: Cooling effect of agricultural irrigation over Xinjiang, Northwest China from 1959 to 2006, Environ. Res. Lett. 8 024039 doi:10.1088/1748-9326/8/2/024039, 2013.

Hasson, S., Gerlitz, L., Scholten, T., Schickhoff, U., and Böhner, J.: Recent Climate Change over High Asia, Springer Book Chapter 2, Dynamics of Climate, Glaciers and

Vegetation in Himalaya: Contribution Towards Future Earth Initiatives, Springer International Publishing AG, Cham, 2015b. (in print)

Hasson, S., Lucarini, V., Pascale, S., and Böhner, J.: Seasonality of the hydrological cycle in major South and Southeast Asian river basins as simulated by PCMDI/CMIP3 experiments, Earth Syst. Dynam., 5, 67–87, doi:10.5194/esd-5-67-2014, 2014a.

Hasson, S., Pascale, S., Lucarini, V., and Böhner, J.: Seasonal cycle of Precipitation over Major River Basins in South and Southeast Asia: A Review of the CMIP5 climate models data for present climate and future climate projections, J. Atmos. Res., 2015a. (Under Review ATMOSRES-D-14-00782)

Hasson, S., Lucarini, V., Khan, M. R., Petitta, M., Bolch, T., and Gioli, G.: Early 21st century snow cover state over the western river basins of the Indus River system, Hydrol. Earth Syst. Sci., 18, 4077-4100, doi:10.5194/hess-18-4077-2014, 2014b.

Heino, R.: Climate in Finland during the Period of Meteorological Observations, Finnish Meteorological Institute Contributions 12, Academic dissertation, Helsinki, 209 pp, 1994.Hasson, S., Lucarini, V., and Pascale, S.: Hydrological cycle over South and Southeast Asian river basins as simulated by PCMDI/CMIP3 experiments, Earth Syst. Dynam., 4, 199–217, doi:10.5194/esd-4-199-2013, 2013.

Hess, A., Lyer, H., Malm, W.: Linear trend analysis: a comparison of methods. Atmos Environ 35:5211–5222, 2001.

Hewitt, K. The Karakoram anomaly? Glacier expansion and the ‘elevation effect’, Karakoram Himalaya. Mt. Res. Dev. 25, 332–340, 2005.

Hewitt, K.: Glacier change, concentration, and elevation effects in the Karakoram Himalaya, Upper Indus Basin, Mt. Res. Dev., 31, 188–200, doi:10.1659/MRD-JOURNAL-D-11-00020.1, 2011.

Hodges, I. K., Hoskins, B. J., Boyle, J., and Thorncroft, C.: A Comparison of Recent Reanalysis Datasets Using Objective Feature Tracking: Storm Tracks and Tropical Easterly Waves, Mon. Weather Rev., 131, 2012–2037, 2003.

Houze, R. A., Rasmussen, K. L., Medina, S., Brodzik, S. R., and Romatschke, U.: Anomalous Atmospheric Events Leading to the Summer 2010 Floods in Pakistan, B. Am. Meteorol. Soc., 92, 291–298, 2011.

Hu, Z. Z., Yang, S., and Wu, R. G.: Long-term climate variations in China and global warming signals. J. Geophys. Res.,108, 4614, doi:10.1029/2003JD003651, 2003.

Huntington, E.: Pangong: a glacial lake in the Tibetan plateau, J. Geol., 14 (7) (1906), pp. 599–617, 1906.

Immerzeel, W. W., Wanders, N., Lutz, A. F., Shea, J. M., and Bierkens, M. F. P.: Reconciling high-altitude precipitation in the upper Indus basin with glacier mass balances and runoff, Hydrol. Earth Syst. Sci., 19, 4673-4687, doi:10.5194/hess-19-4673-2015, 2015

Immerzeel,W.W., Droogers, P., de Jong, S. M., and Bierkens, M. F. P.: Large-scale monitoring of snow cover and runoff simulation in Himalayan river basins using remote sensing, Remote Sens. Environ., 113, 40–49, 2009.

IPCC, 2013: Climate Change 2013: The Physical Science Basis. Contribution ofWorking Group I to the Fifth Assessment Report of the Intergovernmental Panel on Climate Change, edited by: Stocker, T. F., Qin, D., Plattner, G.-K., Tignor, M., Allen, S. K., Boschung, J., Nauels, A., Xia, Y., Bex, V., and Midgley, P. M., Cambridge University Press, Cambridge, United Kingdom and New York, NY, USA, 1535 pp., 2013.

Jaagus, J.: Climatic changes in Estonia during the second half of the 20th century in relationship with changes in large-scale atmospheric circulation. Theor Appl Climatol 83:77–88, 2006.

Jones, P. D., New, M. , Parker, D. E., Martin, S. and Rigor, I. G.: Surface air temperature and its changes over the past 150 years. Rev. Geophys., 37, 173–199, 1999.

Kääb, A., Treichler, D., Nuth, C., and Berthier, E.: Brief Communication: Contending estimates of 2003–2008 glacier mass balance over the Pamir–Karakoram–Himalaya, The Cryosphere, 9, 557-564, doi:10.5194/tc-9-557-2015, 2015.

Kendall, M. G.: Rank Correlation Methods. Griffin, London, UK, 1975.

Khan, A., Richards, K. S., Parker, G. T., McRobie, A., Mukhopadhyay, B.: How large is the Upper Indus Basin? The pitfalls of auto-delineation using DEMs, Journal of Hydrology, 509, 442–453, 2014.

Khattak, M. S., Babel, M. S., and Sharif, M.: Hydrometeorological trends in the upper Indus River Basin in Pakistan, Clim. Res., 46, 103–119, doi:10.3354/cr00957, 2011.

Klein Tank, AMG, Zwiers, FW, Zhang, X.: Guidelines on analysis of extremes in a changing climate in support of informed decisions for adaptation (WCDMP-72, WMO-TD/No.1500), WMO Publications Board, Geneva, Switzerland, 56 pp, 2009.

Kueppers, L. M., M. A. Snyder, and L. C. Sloan, Irrigation cooling effect: Regional climate forcing by land-use change, Geophys. Res. Lett., 34, L03703, doi:10.1029/2006GL028679. 2007.

Kulkarni, A. and von Storch, H.: Monte Carlo experiments on the effect of serial correlation on the Mann–Kendall test of trend. Meteorologische Zeitschrift 4(2): 82–85, 1995.

Kumar, K. R., Kumar, K. K.and Pant, G. B.: Diurnal asymmetry of surface temperature trends over India. Geophys. Res. Lett., 21, 677–680. 1994.

Kumar, S., Merwade, V., Kam, J., Thurner, K.: Streamflow trends in Indiana: effects of long term persistence, precipitation and subsurface drains. J Hydrol (Amst) 374:171–183, 2009.

Kumar, S., Merwade, V., Kinter, J. L., Niyogi, D.: Evaluation of Temperature and Precipitation Trends and Long-Term Persistence in CMIP5 Twentieth-Century Climate Simulations. J. Climate, 26, 4168–4185, 2013.

Lacombe, G., and McCartney, M.: Uncovering consistencies in Indian rainfall trends observed over the last half century, Climatic Change, 123:287–299, 2014.

Liu, X., and Chen, B.: Climatic warming in the Tibetan Plateau during recent decades. Int. J. Climatol., 20, 1729–1742, 2000.

Madhura, R. K., Krishnan, R., Revadekar, J. V., Mujumdar, M., Goswami, B. N.: Changes in western disturbances over the Western Himalayas in a warming environment, Clim Dyn, 44:1157–1168, 2015.

Mann, H. B.: Nonparametric tests against trend, Econometrica 13, 245–259, 1945.

MRI (Mountain Research Initiative) EDW (Elevation Dependent Warming) Working Group: Pepin N, Bradley RS, Diaz HF, Baraer M, Caceres EB, Forsythe N, Fowler H, Greenwood G, Hashmi MZ, Liu XD, Miller JR, Ning L, Ohmura A, Palazzi E, Rangwala I, Schöner W, Severskiy I, Shahgedanova M, Wang MB, Williamson SN, Yang DQ.:

Elevation-dependent warming in mountain regions of the world. Nature Climate Change:5, DOI:10.1038/NCLIMATE2563, 2015.

Mukhopadhyay, B., and Khan, A.: Rising river flows and glacial mass balance in central Karakoram, Journal of Hydrology, 513, 26 Pages 192–203, 2014.

Mukhopadhyay, B., and Khan, A.: A reevaluation of the snowmelt and glacial melt in river flows within Upper Indus Basin and its significance in a changing climate, J. Hydrol., 119-132, 2015.

Mukhopadhyay, B., Khan, A. Gautam, R.: Rising and falling river flows: contrasting signals of climate change and glacier mass balance from the eastern and western Karakoram, Hydrological Sciences Journal, DOI:

10.1080/02626667.2014.947291, 2015.

Ohlendorf, C., Niessenn, F., Weissert, H.:Glacial Varve thickness and 127 years of instrumental climate data: a comparison. Clim. Chang, 36:391–411, 1997.

Palazzi, E., von Hardenberg, J., Provenzale, A.: Precipitation in the Hindu-Kush Karakoram Himalaya: Observations and future scenarios. J Geophys Res Atmos 118:85 {100, DOI 10.1029/2012JD018697, 2013.

Palazzi, E., von Hardenberg, J., Terzago, S., Provenzale, A.: Precipitation in the Karakoram-Himalaya: a CMIP5 view, Climate Dynamics, DOI 10.1007/s00382-014-2341-z, 2014.

Peterson, T. C., Easterling, D. R., Karl, T. R., Groisman, P., Nicholls, C., Plummer, N., Torok, S., Auer, I, Boehm, R., Gullett, D., Vincent, L., Heino, R., Tuomenvarta, H., Mestre, O., Szentimrey, T., Salinger, J., FØrland, E. J., Hanssen-Bauer, I, Alexandersson, H., Jonesi, P., and Parker, D.: Homogeneity Adjustments of In Situ Atmospheric Climate Data: A Review, Int. J. Climatol., 18: 1493–1517, 1998.

Rees, H. G. and Collins, D. N.: Regional differences in response of flow in glacier-fed Himalayan rivers to climatic warming, Hydrol. Process., 20, 2157–2169, 2006.

Reggiani, P. & Rientjes, T. H. M.: A reflection on the long-term water balance of the Upper Indus Basin. Hydrology Research:1-17, 2014

Revadekar, J. V., Hameed, S., Collins, D., Manton, M., Sheikh, M., Borgaonkar, H. P., Kothawale, D. R., Adnan, M., Ahmed, A. U., Ashraf, J., Baidya, S., Islam, N., Jayasinghearachchi, D., Manzoor, N., Premalal, K. H. M. S. and Shreshta, M. L, Impact of altitude and latitude on changes in temperature extremes over South Asia during 1971–2000. Int. J. Climatol., 33: 199–209. doi: 10.1002/joc.3418. 2013.

Ridley, J., Wiltshire, A., and Mathison, C.:More frequent occurrence of westerly disturbances in Karakoram up to 2100, Science of The Total Environment, 468–469, S31–S35, 2013.

Río, S. D., Iqbal, M. A., Cano-Ortiz, A., Herrero, L., Hassan, A. and Penas, A.: Recent mean temperature trends in Pakistan and links with teleconnection patterns. Int. J. Climatol., 33: 277–290. doi: 10.1002/joc.3423, 2013

Rivard, C. and Vigneault, H.: Trend detection in hydrological series: when series are negatively correlated, Hydrol. Process. 23, 2737–2743, 2009.

Salik, K. M., Jahangir, S., Zahdi, W. Z., and Hasson, S.: Climate change vulnerability and adaptation options for the coastal communities of Pakistan, Ocean & Coastal Management, under review article # OCMA-D-14-00289, 2015.

Scherler, D., Bookhagen, B., Strecker, M. R.: Spatially variable response of Himalayan glaciers to climate change affected by debris cover. Nat. Geosci. 4, Nature Geoscience 4, 156–159, doi:10.1038/ngeo1068, 2011.

Sen, P. K.: Estimates of the regression coefficient based on Kendall's tau. J. Am. Statist. Assoc. 63, 1379–1389, 1968.

Shaman, J. and Tziperman, E.: The Effect of ENSO on Tibetan Plateau Snow Depth: A Stationary Wave Teleconnection Mechanism and Implications for the South Asian Monsoons, J. Climtol., 18, 2067–2079, 2005.

Sharma, K. P., Moore, B.and Vorosmarty, C. J.: Anthropogenic, climatic and hydrologic trends in the Kosi basin, Himalaya. Climatic Change, 47, 141–165, 2000.

Sheikh, M. M., Manzoor, N., Adnan, M., Ashraf, J., and Khan, A. M.: Climate Profile and Past Climate Changes in Pakistan, GCISC-RR-01, Global Change Impact Studies Centre (GCISC), Islamabad, Pakistan, ISBN: 978-969-9395-04-8, 2009.

Shrestha, A. B., C. Wake, P. A. Mayewski, and J. Dibb,: Maximum temperature trends in the Himalaya and its vicinity: An analysis based on temperature records from Nepal for the period 1971–94. J. Climate, 12, 2775–2786, 1999.

SIHP: Snow and Ice Hydrology, Pakistan Phase-II Final Report to CIDA, IDRC File No. 88-8009-00 International Development Research Centre, Ottawa, Ontario, Canada, KIG 3H9, Report No. IDRC.54, 1997.

Syed, F. S., Giorgi, F., Pal, J. S., and King, M. P.: Effect of remote forcing on the winter precipitation of central southwest Asia Part 1: Observations, Theor. Appl. Climatol., 86, 147–160, doi:10.1007/s00704-005-0217-1, 2006.

Tabari, H., and Talaee, P. H.: Recent trends of mean maximum and minimum air temperatures in the western half of Iran, Meteorol. Atmos. Phys.,111:121–131, 2011.

Tahir, A.A.: Impact of climate change on the snow covers and glaciers in the Upper Indus River Basin and its consequences on the water reservoirs (Tarbela Dam) – Pakistan. UNIVERSITE MONTPELLIER 2. 2011.

Theil, H.: A rank-invariant method of linear and polynomial regression analysis, I, II, III. Nederl. Akad. Wetensch, Proc. 53, 386–392, 512–525, 1397–1412, Amsterdam, 1950.

Thompson, D. W. J. and Wallace, J. M.: Regional climate impacts of the Northern Hemisphere Annular Mode Science 293 85–9, 2001.

Thompson, D. W. J. and Wallace, J. M.: The Arctic Oscillation signature in the wintertime geopotential height and temperature fields Geophys. Res. Lett. 25 1297–300, 1998.

Vogel, R.M., and Kroll, C.N.: Low-flow frequency analysis using probability plot correlation coefficients, J. Water Res. Plann. Mgmt, 115 (3) (1989), pp. 338–357, 1989.

Von Storch, H.: Misuses of statistical analysis in climate research. In Analysis of Climate Variability: Applications of Statistical Techniques, von Storch H, Navarra A (eds). Springer-Verlag: Berlin; 11–26, 1995.

Wake, C. P.: Glaciochemical investigations as a tool to determine the spatial variation of snow accumulation in the Central Karakoram, Northern Pakistan, Ann. Glaciol., 13, 279–284, 1989.

Wake, C. P.: Snow accumulation studies in the central Karakoram, Proc. Eastern Snow Conf. 44th Annual Meeting Fredericton, Canada, 19–33, 1987.

Wang XL, Feng Y.: RHtestsV3 user manual, report, 26 pp, Clim. Res. Div., Atmos. Sci. and Technol. Dir., Sci. and Technol. Branch, Environ. Canada, Gatineau, Quebec, Canada. Available at http://etccdi.pacificclimate.org/software.shtml, (last access: 15 November 2014), 2009.

Wang, F., Zhang, C., Peng, Y. and Zhou, H.: Diurnal temperature range variation and its causes in a semiarid region from 1957 to 2006. Int. J. Climatol., 34: 343–354. doi: 10.1002/joc.3690, 2014.

Wang, X. L. and Swail, V. R.: Changes of Extreme Wave Heights in Northern Hemisphere Oceans and Related Atmospheric Circulation Regimes, J. Clim., 14, 2204-2221, 2001.

Wang, X. L.: Penalized maximal F-test for detecting undocumented mean shifts without trend-change. J. Atmos. Oceanic Tech., 25 (No. 3), 368-384. DOI:10.1175/2007JTECHA982.12008.

Wendler, G. and Weller, G.: ‘A Heat-Balance Study on McCall Glacier, Brooks Range, Alaska: A Contribution to the International Hydrological Decade’, J. Glaciol. 13, 13–26. 1974.

Winiger, M., Gumpert, M., and Yamout, H.: Karakorum–Hindukush–western Himalaya: assessing high-altitude water resources, Hydrol. Process., 19, 2329–2338, doi:10.1002/hyp.5887, 2005.

Wu, H., Soh, L-K., Samal, A., Chen, X-H: Trend Analysis of Streamflow Drought Events n Nebraska, Water Resour. Manage., DOI 10.1007/s11269-006-9148-6, 2008.

Yadav, R. R., Park, W.-K., Singh, J. and Dubey, B.: Do the western Himalayas defy global warming? Geophys. Res. Lett., 31, L17201, doi:10.1029/2004GL020201. 2004.

Yue S, Hashino M. Long term trends of annual and monthly precipitation in Japan. Journal of the American Water Resources Association 39: 587–596.2003.

Yue, S. and Wang, C. Y.: Regional streamflow trend detection with consideration of both temporal and spatial correlation. Int. J. Climatol., 22: 933–946. doi: 10.1002/joc.781. 2002.

Yue, S., Pilon, P., Phinney, B. and Cavadias, G.: The influence of autocorrelation on the ability to detect trend in hydrological series, Hydrol. Process. 16, 1807–1829, 2002.

Yue, S., Pilon, P., Phinney, B.: Canadian streamflow trend detection: impacts of serial and cross-correlation, Hydrological Sciences Journal, 48:1, 51-63, DOI: 10.1623/hysj.48.1.51.43478, 2003.

Zhai, P. Zhang, X., Wan, H., and Pan, X.: Trends in Total Precipitation and Frequency of Daily Precipitation Extremes over China. J. Climate, 18, 1096–1108, 2005. doi: http://dx.doi.org/10.1175/JCLI-3318.1

Zhang, X., Vincent, L. A., Hogg, W.D. and Niitsoo, A.: Temperature and precipitation trends in Canada during the 20th century, Atmosphere-Ocean, 38:3, 395-429, 2000.

Table 1: Characteristics of the gauged and derived regions of UIB. Note: *Including nearby Skardu and Gilgit stations for the Karakoram and Deosai station for the UIB-Central regions. Derived gauge times series are limited to common length of time series of the employed gauges, thus their statistics.

S. No.	Watershed/ Tributary	Designated Discharge sites	Expression for deriving approximated Discharge	Designated Name of the Region	Area (km^2)	Glacier Cover (km^2)	% Glacier Cover	% of UIB Glacier Aboded	Elevation Range (m)	Mean Discharge (m^3s^{-1})	% of UIB Discharge	No of Met Stations
1	Indus	Kharmong		UIB-East	69,355	2,643	4	14	2250-7027	451	18.8	1
2	Shyok	Yogo		Eastern-Karakoram	33,041	7,783	24	42	2389-7673	360	15.0	1
3	Shigar	Shigar		Central-Karakoram	6,990	2,107	30	11	2189-8448	206	8.6	1
4	Indus	Kachura		Indus at Kachura	113,035	12,397	11	68	2149-8448	1078	44.8	
5	Hunza	Dainyor Bridge		Western-Karakoram	13,734	3,815	28	21	1420-7809	328	13.6	4
6	Gilgit	Gilgit		Hindukush	12,078	818	7	4	1481-7134	289	12.0	5
7	Gilgit	Alam Bridge		UIB-West-upper	27,035	4,676	21	25	1265-7809	631	27.0	9
8	Indus	Partab Bridge		Indus at Partab	143,130	17,543	12	96	1246-8448	1788	74.3	
9	Astore	Doyian		Astore at Doyian	3,903	527	14	3	1504-8069	139	5.8	3
10	**UIB**	**Besham Qila**		**UIB**	**163,528**	**18,340**	**11**	**100**	**569-8448**	**2405**	**100.0**	**18**
11			4 – 2 – 1	Shigar-region						305	12.7	
12			2 + 3 + 5	Karakoram	53,765	13,705	25	75	1420-8448	894	37.2	*8
13			2 + 11 + 5	derived Karakoram						993	41.3	
14			4 – 1	UIB-Central	43,680	9,890	23	54	2189-8448	627	26.1	*4
15			10 – 4	UIB-West	50,500	5,817	13	32	569-7809	1327	55.2	14
16			10 – 4 – 7	UIB-West-lower	23,422	1,130	7	6	569-8069	696	28.9	5
17			1 + 16	Himalaya	92,777	3,773	5	20	569-8069	1147	47.7	7

Table 2: List of Meteorological Stations and their attributes. Inhomogeneity is found only in Tn over full period of record. Note: (*) represent inhomogeneity for 1995-2012 period only.

S.	**Station Name**	**Period From**	**Period To**	**Agency**	**Longitude**	**Latitude**	**Altitude**	**Inhomogeneity at**
1	Chillas	01/01/1962	12/31/2012	PMD	35.42	74.10	1251	2009/03
2	Bunji	01/01/1961	12/31/2012	PMD	35.67	74.63	1372	1977/11
3	Skardu	01/01/1961	12/31/2012	PMD	35.30	75.68	2210	
4	Astore	01/01/1962	12/31/2012	PMD	35.37	74.90	2168	1981/08
5	Gilgit	01/01/1960	12/31/2012	PMD	35.92	74.33	1460	2003/10*
6	Gupis	01/01/1961	12/31/2010	PMD	36.17	73.40	2156	1988/12 1996/07*
7	Khunjrab	01/01/1995	12/31/2012	WAPDA	36.84	75.42	4440	
8	Naltar	01/01/1995	12/31/2012	WAPDA	36.17	74.18	2898	2010/09*
9	Ramma	01/01/1995	09/30/2012	WAPDA	35.36	74.81	3179	
10	Rattu	03/29/1995	03/16/2012	WAPDA	35.15	74.80	2718	
11	Hushe	01/01/1995	12/31/2012	WAPDA	35.42	76.37	3075	
12	Ushkore	01/01/1995	12/31/2012	WAPDA	36.05	73.39	3051	
13	Yasin	01/01/1995	10/06/2010	WAPDA	36.40	73.50	3280	
14	Ziarat	01/01/1995	12/31/2012	WAPDA	36.77	74.46	3020	
15	Dainyor	01/15/1997	07/31/2012	WAPDA	35.93	74.37	1479	
16	Shendoor	01/01/1995	12/28/2012	WAPDA	36.09	72.55	3712	
17	Deosai	08/17/1998	12/31/2011	WAPDA	35.09	75.54	4149	
18	Shigar	08/27/1996	12/31/2012	WAPDA	35.63	75.53	2367	

Table 3. List of SWHP WAPDA Stream flow gauging stations in a downstream order along with their characteristics and period of record used**. ***Gauge is not operational after 2001.

S. No.	**Gauged River**	**Discharge Gauging Site**	**Period From**	**Period To**	**Degree Latitude**	**Degree Longitude**	**Height meters**
1	Indus	Kharmong	May-82	Dec-11	34.9333333	76.2166667	2542
2	Shyok	Yogo	Jan-74	Dec-11	35.1833333	76.1000000	2469
3	Shigar	Shigar*****	Jan-85	Dec-98 & 2001	35.3333333	75.7500000	2438
4	Indus	Kachura	Jan-70	Dec-11	35.4500000	75.4166667	2341
5	Hunza	Dainyor	Jan-66	Dec-11	35.9277778	74.3763889	1370
6	Gilgit	Gilgit	Jan-70	Dec-11	35.9263889	74.3069444	1430
7	Gilgit	Alam Bridge	Jan-74	Dec-12	35.7675000	74.5972222	1280
8	Indus	Partab Bridge	Jan-62	Dec-07	35.7305556	74.6222222	1250
9	Astore	Doyian	Jan-74	Aug-11	35.5450000	74.7041667	1583
10	UIB	Besham Qila	Jan-69	Dec-12	34.9241667	72.8819444	580

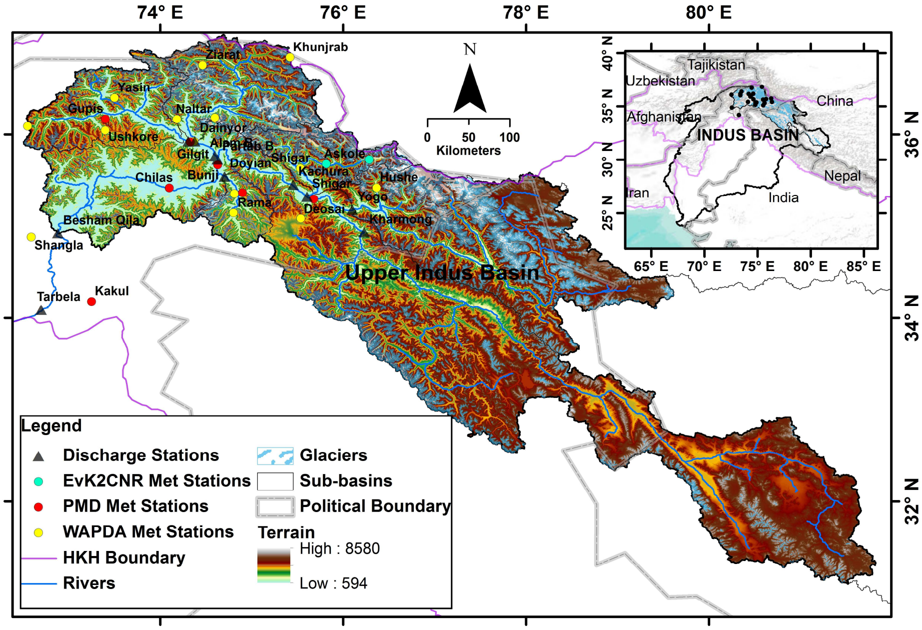

Figure 1: Study Area, Upper Indus Basin (UIB) and meteorological station networks

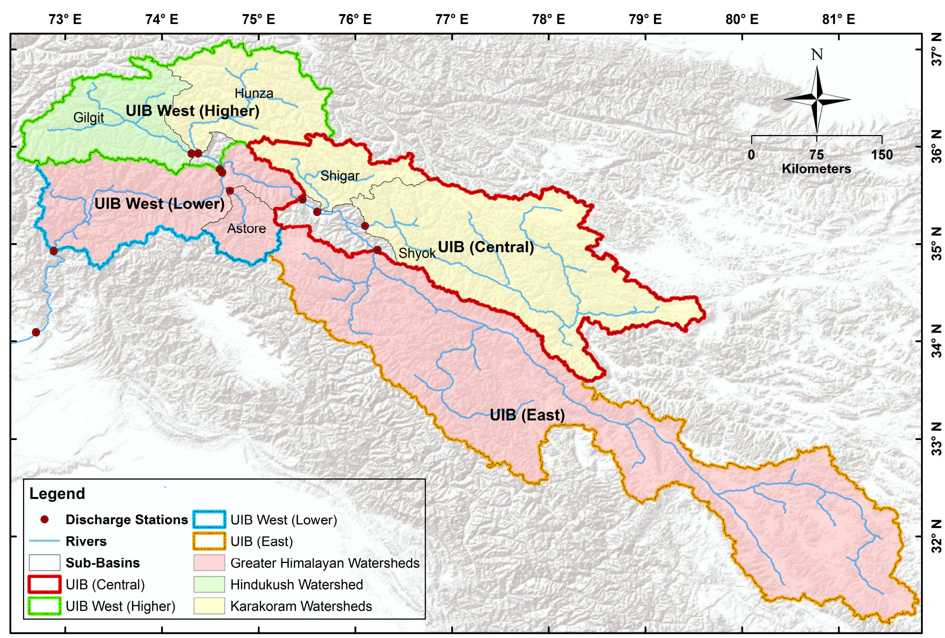

Figure 2: Gauged basins, gauges and regions considered for field significance

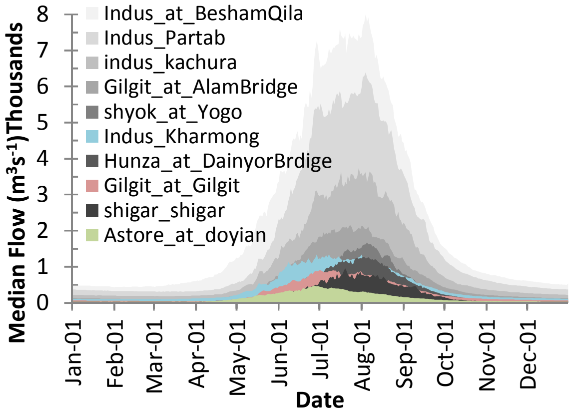

Figure 3: Long-term median hydrograph for ten key gauging stations separating the sub-basins of UIB having either mainly snow-fed (shown in color) or mainly glacier-fed hydrological regimes (shown in grey shades).

Tabular Figure 4: Trend for Tx, Tn and DTR in $^{o}C\ yr^{-1}$ (per unit time) at monthly to annual time scale over the period 1995-2012. Note: meteorological stations are ordered from top to bottom as highest to lowest altitude while hydrometric stations as upstream to downstream. Slopes significant at 90% level are given in bold while at 95% are given in bold and Italic. Color scale is distinct for each time scale where blue (red) refers to increasing (decreasing) trend

Variable	Stations	Jan	Feb	Mar	Apr	May	Jun	Jul	Aug	Sep	Oct	Nov	Dec	DJF	MAM	JJA	SON	Ann.
Tx	Khunrab	0.01	-0.01	0.10	0.03	0.12	-0.01	-0.09	0.06	-0.16	0.01	0.12	0.07	0.05	0.07	-0.05	0.04	0.04
	Deosai	0.02	-0.05	0.07	-0.01	0.06	0.01	-0.19	-0.01	0.00	0.02	0.06	0.05	0.08	0.06	0.03	0.02	0.06
	Shendure	-0.17	**-0.09**	0.01	-0.03	-0.06	-0.10	**-0.13**	***-0.07***	***-0.22***	-0.06	0.04	-0.11	-0.08	-0.06	**-0.11**	-0.05	-0.05
	Yasin	0.00	-0.03	**0.13**	-0.02	0.10	0.03	-0.16	-0.08	***-0.35***	0.12	-0.02	-0.10	0.03	0.08	-0.06	-0.01	0.05
	Rama	-0.06	-0.07	0.02	**-0.11**	0.14	0.04	-0.11	-0.09	**-0.29**	-0.10	0.01	0.00	-0.04	-0.04	**-0.07**	-0.07	***-0.08***
	Hushe	-0.05	-0.01	0.09	0.00	0.17	-0.06	-0.09	0.02	**-0.20**	-0.09	0.01	0.03	0.02	0.03	-0.02	-0.03	-0.03
	Ushkore	-0.04	-0.02	0.10	0.03	0.25	-0.01	-0.12	-0.06	***-0.22***	-0.05	0.06	-0.01	0.02	0.08	-0.05	-0.02	-0.01
	Ziarat	0.00	-0.01	0.12	-0.02	0.13	0.09	-0.11	-0.03	***-0.21***	-0.04	0.09	0.04	0.06	0.06	-0.02	-0.04	0.01
	Naltar	-0.04	-0.04	0.10	-0.03	0.10	0.03	-0.12	-0.03	***-0.19***	0.03	-0.01	0.01	-0.02	0.07	-0.03	-0.05	0.00
	Rattu	***-0.16***	-0.10	0.04	-0.03	0.11	0.14	-0.06	-0.05	-0.17	-0.23	0.04	-0.15	***-0.12***	-0.03	0.01	-0.03	**-0.07**
	Shigar	-0.04	-0.08	-0.02	-0.08	-0.38	-0.15	-0.08	0.03	-0.01	-0.09	0.11	0.01	-0.02	-0.09	**-0.09**	-0.02	-0.02
	Skardu	0.10	0.08	0.12	0.04	0.04	-0.08	**-0.10**	0.06	***-0.23***	-0.10	-0.04	-0.05	-0.02	0.13	-0.07	***-0.09***	-0.02
	Astore	0.09	0.00	**0.20**	0.03	0.18	0.06	-0.05	-0.03	***-0.15***	-0.11	0.05	0.04	0.08	**0.15**	-0.01	-0.05	0.02
	Gupis	-0.05	0.03	***0.27***	0.11	0.20	0.01	-0.09	-0.13	-0.09	0.12	0.12	0.03	0.11	0.20	0.03	0.03	0.07
	Dainyor	-0.04	-0.08	***0.23***	-0.02	0.15	-0.19	***-0.18***	0.01	-0.15	-0.04	0.10	-0.07	**-0.06**	0.14	-0.08	-0.01	-0.02
	Gilgit	0.09	-0.07	0.12	0.03	0.15	0.02	**-0.15**	**-0.08**	***-0.31***	-0.07	0.07	-0.05	-0.04	0.06	-0.05	***-0.08***	-0.05
	Bunji	0.09	-0.08	0.13	0.04	0.11	0.07	-0.01	0.04	***-0.22***	-0.12	-0.01	-0.08	0.00	0.11	0.02	-0.07	-0.02
	Chilas	0.09	-0.03	**0.16**	0.01	0.13	0.01	**-0.15**	-0.06	***-0.24***	0.00	0.03	-0.06	-0.05	0.08	**-0.07**	-0.05	-0.06
Tn	Khunrab	***0.15***	***0.26***	**0.16**	0.03	0.18	-0.02	-0.04	0.00	0.01	0.05	***0.17***	0.10	***0.21***	0.08	-0.01	0.06	**0.09**
	Deosai	0.02	0.09	**0.21**	0.00	0.01	0.00	0.03	-0.02	-0.08	0.03	0.09	0.00	0.06	0.10	-0.02	0.05	**0.10**
	Shendure	0.04	-0.03	0.10	0.06	0.05	0.00	**-0.06**	0.00	-0.10	-0.01	0.10	0.08	0.09	0.07	-0.03	0.01	0.05
	Yasin	0.09	0.07	0.12	0.02	0.10	0.01	-0.11	-0.05	***-0.21***	0.10	0.04	-0.08	0.06	**0.11**	-0.04	0.03	***0.08***
	Rama	-0.08	0.10	0.05	0.02	0.06	0.01	0.00	0.01	-0.09	0.00	0.11	0.07	-0.02	0.03	0.03	0.02	0.02
	Hushe	0.00	**0.14**	0.08	0.02	0.14	-0.04	-0.08	0.04	**-0.09**	-0.04	0.04	0.01	0.06	0.06	-0.01	0.01	0.01
	Ushkore	-0.06	0.05	0.08	0.09	0.13	0.00	-0.04	-0.02	***-0.16***	-0.09	0.08	0.01	0.00	0.08	0.01	-0.01	0.00
	Ziarat	0.12	***0.23***	0.11	0.04	0.04	0.04	**-0.08**	0.01	**-0.10**	-0.01	0.09	0.09	***0.17***	0.07	0.00	0.01	***0.06***
	Naltar	-0.01	0.08	0.10	0.02	-0.01	-0.03	**-0.10**	-0.01	**-0.07**	0.00	-0.03	0.00	-0.07	0.10	-0.03	-0.01	0.04
	Rattu	-0.05	0.10	-0.08	-0.02	0.06	0.05	-0.07	0.01	-0.12	-0.02	0.07	0.01	0.04	-0.03	0.01	**-0.08**	-0.04
	Shigar	0.03	0.02	-0.01	-0.03	-0.21	-0.09	-0.07	0.05	0.07	-0.11	0.05	0.04	0.01	-0.02	-0.06	-0.01	0.01
	Skardu	-0.03	0.08	-0.02	-0.02	-0.07	-0.11	-0.15	-0.08	-0.10	***-0.12***	***-0.14***	-0.11	-0.18	-0.01	**-0.12**	***-0.16***	***-0.08***
	Astore	0.01	0.09	0.05	0.03	-0.02	0.02	-0.07	0.01	**-0.10**	-0.05	0.05	-0.08	0.06	**0.11**	-0.01	-0.03	-0.02
	Gupis	-0.15	-0.03	**0.19**	0.11	0.09	0.03	-0.04	0.04	-0.07	-0.03	-0.12	-0.14	-0.11	0.14	-0.04	-0.09	0.01
	Dainyor	-0.13	0.01	***0.13***	0.01	0.11	-0.04	***-0.17***	**0.03**	-0.06	-0.02	-0.06	-0.05	0.01	0.07	-0.03	-0.04	0.01
	Gilgit	0.03	0.10	0.06	0.04	0.04	0.05	-0.01	**0.26**	**0.30**	0.05	0.09	-0.01	0.08	***0.07***	0.06	0.19	**0.08**
	Bunji	0.01	0.03	0.05	0.03	0.02	0.04	-0.01	0.17	0.01	0.03	**0.13**	0.00	0.02	0.05	0.06	0.04	0.03
	Chilas	-0.09	***-0.18***	0.01	-0.07	0.02	-0.05	-0.11	-0.08	**-0.21**	-0.10	0.00	-0.06	-0.15	-0.05	**-0.07**	***-0.11***	-0.07
DTR	Khunrab	-0.10	***-0.25***	-0.30	-0.19	***-0.24***	-0.08	***-0.13***	**-0.11**	***-0.11***	-0.04	-0.03	-0.05	***-0.17***	-0.18	-0.04	***-0.04***	***-0.08***
	Deosai	0.07	-0.09	0.01	0.11	-0.05	0.05	0.16	***0.19***	0.01	0.02	-0.01	0.03	0.01	0.00	0.13	0.01	***0.13***
	Shendure	-0.06	-0.09	-0.26	***-0.29***	-0.17	-0.08	-0.03	-0.05	***-0.09***	-0.07	-0.05	-0.24	-0.12	**-0.20**	-0.10	-0.06	-0.15
	Yasin	-0.13	**-0.23**	-0.05	***-0.15***	-0.12	***-0.20***	-0.13	-0.11	***-0.22***	***-0.58***	-0.24	-0.19	**-0.08**	-0.07	**-0.14**	***-0.25***	**-0.12**
	Rama	-0.05	***-0.16***	-0.04	***-0.11***	-0.04	-0.02	***-0.15***	***-0.13***	***-0.27***	-0.20	-0.08	-0.07	***-0.09***	-0.07	***-0.07***	***-0.13***	***-0.08***
	Hushe	***-0.08***	***-0.17***	-0.01	-0.05	-0.02	0.00	-0.03	-0.02	***-0.07***	0.00	-0.03	-0.01	***-0.10***	-0.01	-0.02	***-0.03***	***-0.04***
	Ushkore	0.00	-0.06	-0.02	-0.08	-0.01	-0.05	-0.01	-0.02	***-0.08***	-0.01	-0.02	-0.03	-0.03	-0.02	-0.03	**-0.03**	***-0.03***
	Ziarat	-0.09	***-0.26***	0.02	-0.02	0.01	-0.01	-0.05	-0.01	***-0.10***	-0.03	-0.03	-0.12	-0.13	0.03	-0.02	**-0.05**	***-0.06***
	Naltar	-0.06	***-0.15***	0.02	-0.06	0.06	-0.02	-0.02	-0.02	-0.09	-0.03	-0.03	-0.13	***-0.08***	0.00	-0.01	-0.06	**-0.05**
	Rattu	-0.10	**-0.16**	-0.04	**-0.10**	0.02	-0.04	-0.09	***-0.11***	***-0.18***	***-0.16***	-0.18	**-0.15**	***-0.12***	-0.01	**-0.04**	-0.10	**-0.05**
	Shigar	0.08	0.00	-0.05	0.00	0.01	0.03	-0.03	-0.01	-0.07	0.01	**0.08**	0.07	0.07	0.03	-0.06	0.00	-0.07
	Skardu	-0.04	**-0.14**	0.06	0.01	**0.13**	0.06	-0.01	-0.02	***-0.21***	0.04	0.03	0.14	-0.07	0.07	-0.01	-0.01	0.00
	Astore	-0.02	-0.13	0.13	0.00	0.05	0.00	-0.03	-0.07	***-0.08***	0.03	-0.03	0.04	-0.09	0.06	-0.02	-0.05	-0.01
	Gupis	0.04	0.00	0.15	-0.01	0.10	-0.01	-0.03	-0.10	-0.05	**0.16**	0.16	0.15	***0.13***	0.07	-0.06	0.09	0.09
	Dainyor	-0.05	-0.09	0.06	-0.11	-0.21	-0.19	-0.11	-0.07	-0.10	-0.44	-0.01	-0.07	-0.09	-0.07	-0.23	-0.12	-0.19
	Gilgit	-0.13	**-0.19**	0.05	-0.02	0.10	-0.13	***-0.27***	***-0.26***	***-0.87***	-0.18	-0.09	-0.02	-0.11	-0.03	***-0.15***	***-0.25***	***-0.18***
	Bunji	-0.04	***-0.14***	0.05	0.03	0.04	-0.01	-0.03	-0.04	**-0.27**	-0.03	-0.16	-0.10	-0.07	0.06	-0.01	***-0.14***	-0.05
	Chilas	0.07	0.09	***0.21***	0.11	**0.13**	0.03	-0.04	0.04	0.00	0.08	0.01	0.04	0.10	***0.14***	0.02	0.02	0.02

Tabular Figure 5: Same as Table 4 but trend slopes are for Tavg in $^{o}C\ yr^{-1}$, for total P in mm yr^{-1} and for mean Q in $m^3s^{-1}yr^{-1}$. Color scale is distinct for each time scale where blue, yellow and orange (red, green and cyan) colors refer to decrease (increase) in Tavg, P and Q, respectively

Variable	Stations	Jan	Feb	Mar	Apr	May	Jun	Jul	Aug	Sep	Oct	Nov	Dec	DJF	MAM	JJA	SON	Ann.
Tavg	Khunrab	0.13	0.09	0.13	0.05	0.19	0.00	-0.06	0.06	-0.13	0.05	***0.17***	0.10	***0.15***	0.09	-0.03	0.06	0.06
	Deosai	0.06	0.01	**0.15**	0.00	0.07	0.01	-0.07	0.03	-0.05	0.02	0.08	0.01	***0.10***	0.06	0.03	0.04	**0.07**
	Shendure	-0.05	-0.05	0.05	0.02	0.02	-0.05	-0.10	-0.05	**-0.15**	-0.04	0.06	-0.03	0.01	-0.04	-0.05	-0.02	0.01
	Yasin	0.02	0.01	**0.13**	0.01	0.06	0.04	-0.19	-0.07	***-0.27***	0.11	0.01	-0.08	0.04	0.13	-0.05	0.02	0.06
	Rama	-0.12	0.02	0.05	-0.06	0.07	0.01	-0.03	-0.03	**-0.19**	-0.09	0.05	0.02	0.02	0.00	0.00	-0.01	-0.04
	Hushe	-0.03	0.05	0.06	0.02	0.14	-0.05	-0.07	0.02	**-0.13**	-0.07	0.03	0.04	0.01	0.06	-0.01	0.00	-0.01
	Ushkore	-0.07	0.00	0.08	0.05	0.21	0.00	-0.03	-0.03	***-0.17***	-0.09	0.06	0.01	0.04	0.09	-0.01	-0.02	0.01
	Ziarat	0.04	***0.11***	0.10	0.00	0.09	0.06	-0.09	-0.03	***-0.15***	-0.03	0.09	0.03	**0.08**	**0.07**	-0.02	0.00	0.05
	Naltar	-0.03	0.01	0.08	-0.05	-0.11	-0.07	**-0.12**	-0.06	***-0.17***	0.00	-0.03	0.01	-0.13	0.07	-0.04	-0.04	0.01
	Rattu	-0.11	-0.01	-0.05	-0.04	0.09	0.10	-0.04	0.00	-0.18	-0.07	0.04	-0.10	-0.06	0.03	0.00	-0.05	-0.05
	Shigar	0.05	-0.02	0.00	-0.06	-0.30	-0.13	-0.13	0.04	0.04	-0.14	0.07	0.03	0.01	-0.04	-0.07	-0.01	0.00
	Skardu	0.02	0.11	0.07	0.01	0.02	-0.10	***-0.15***	0.04	***-0.17***	***-0.11***	**-0.06**	-0.07	-0.11	0.06	-0.12	***-0.12***	**-0.07**
	Astore	0.10	0.03	**0.12**	0.01	0.13	0.03	-0.05	0.00	***-0.14***	-0.09	0.03	-0.01	0.05	**0.13**	-0.02	-0.03	0.01
	Gupis	-0.08	-0.06	***0.22***	0.09	0.13	0.00	-0.05	-0.05	-0.08	0.06	0.04	-0.07	0.02	**0.14**	0.02	-0.01	0.03
	Dainyor	-0.06	-0.02	***0.22***	-0.01	0.18	-0.08	***-0.15***	0.02	-0.11	-0.04	0.04	-0.09	-0.05	0.11	-0.04	-0.04	0.00
	Gilgit	0.02	0.01	0.11	0.03	0.06	0.04	-0.06	0.05	-0.09	0.00	***0.08***	0.05	0.03	0.08	-0.02	0.00	0.03
	Bunji	0.06	-0.02	0.06	0.02	0.05	0.02	0.00	0.09	-0.07	0.03	0.06	-0.06	0.03	0.08	0.06	0.00	0.01
	Chilas	-0.02	-0.14	0.06	-0.02	0.16	-0.03	**-0.12**	-0.07	**-0.19**	-0.07	0.01	-0.06	***-0.09***	0.03	**-0.06**	**-0.08**	-0.07
P	Khunrab	***3.64***	2.59	-2.21	-1.55	-1.47	0.10	0.35	0.80	1.82	-1.04	0.93	2.34	***8.86***	-9.09	-1.74	1.65	6.14
	Deosai	0.07	1.28	**-1.42**	-0.66	-1.27	-0.89	-0.40	-1.00	-0.77	-0.42	-0.81	-0.32	1.40	-4.50	0.00	-1.99	-7.87
	Shendure	***1.54***	***2.75***	1.35	2.13	0.60	***2.12***	***1.83***	***1.38***	***1.45***	1.24	1.40	***1.20***	***5.71***	***4.50***	***4.82***	**3.58**	***29.53***
	Yasin	1.33	***1.86***	0.59	0.25	1.22	-0.50	***1.45***	0.02	0.92	-0.21	0.06	**2.74**	***6.09***	0.60	1.32	0.26	11.70
	Rama	0.77	0.00	-6.50	***-8.55***	***-4.52***	***-2.16***	***-2.35***	***-1.89***	***-1.44***	***-2.05***	-3.74	-2.03	7.00	***-25.44***	***-8.41***	***-14.60***	***-43.92***
	Hushe	0.65	0.24	-1.23	-0.30	-1.97	-1.21	-1.71	-0.60	0.73	-0.64	0.11	0.72	***3.47***	-4.51	-4.28	0.70	-5.54
	Ushkore	0.56	-0.59	***-2.33***	-1.02	-1.97	-0.93	0.00	-0.09	1.01	***-0.61***	-0.48	0.09	-0.13	-4.57	-1.54	-0.42	-3.83
	Ziarat	-0.91	-0.56	***-4.18***	**-5.28**	-1.83	0.25	-0.67	-0.18	**1.20**	-0.58	-0.43	-0.61	-3.59	**-9.10**	-1.71	-0.21	**-16.32**
	Naltar	3.75	8.41	-4.49	-0.36	-2.75	**-2.17**	0.43	-2.33	1.32	-0.36	-0.70	1.35	**19.43**	-8.39	-0.99	2.42	-0.28
	Rattu	***1.36***	**2.13**	0.08	0.36	0.26	0.53	***0.91***	0.75	***0.95***	***0.84***	***0.69***	***1.53***	***4.43***	1.23	1.81	***2.36***	10.64
	Shigar	-0.24	-0.89	-1.07	-2.62	-2.05	-0.33	1.75	0.80	***2.40***	1.13	0.18	1.49	-1.67	**-8.36**	0.78	**3.08**	-7.04
	Skardu	-0.64	1.62	0.60	0.19	-0.74	-0.47	-0.07	-0.44	0.46	0.00	0.00	0.20	0.41	0.89	-1.26	0.49	1.29
	Astore	0.00	0.41	0.12	**-1.41**	-0.48	-0.16	-0.08	-0.29	0.57	0.00	0.00	0.29	1.50	-1.36	-1.63	0.34	-0.16
	Gupis	0.65	**0.97**	**0.81**	0.38	-0.06	**-1.33**	**-1.07**	-0.49	0.06	0.35	0.26	***0.89***	2.81	0.29	***-3.49***	0.43	4.46
	Dainyor	-0.21	0.42	***0.51***	**0.55**	***0.67***	***1.24***	0.91	-0.71	-0.39	0.00	0.00	0.00	***1.68***	**1.81**	3.09	-0.34	6.69
	Gilgit	0.98	0.45	**-1.94**	-1.34	-1.57	-0.73	0.29	***-3.99***	0.32	0.00	0.00	0.30	0.00	***-9.39***	***-9.60***	-0.92	**-20.31**
	Bunji	0.01	-0.10	***-1.06***	***-2.34***	0.17	0.20	-0.34	-0.22	0.56	-0.01	0.00	0.11	-0.47	-2.68	-0.51	0.06	0.09
	Chilas	0.00	0.13	-0.14	-1.56	0.16	0.29	-0.51	0.13	***1.37***	-0.10	0.00	0.07	0.22	-0.81	-0.80	1.86	0.53
Q	UIB-East	***-0.80***	0.00	0.04	0.11	-4.19	2.00	-1.65	6.70	-4.74	-5.45	***-2.46***	**-1.37**	***-0.75***	-2.64	-2.62	-0.86	-1.73
	Eastern-Karakoram	0.06	0.08	-0.10	0.00	1.96	0.96	**-22.97**	0.92	-8.84	-1.06	0.50	-0.09	0.29	0.67	0.30	-4.41	-0.95
	Central-Karakoram	0.96	1.28	1.56	-0.84	3.74	-8.94	***-37.93***	-9.08	-5.98	0.71	2.50	***2.76***	1.13	1.13	-21.61	1.10	-1.56
	Kachura	0.33	1.39	**1.06**	-0.33	-2.08	-22.50	**-50.04**	-16.74	-4.25	-2.18	0.59	2.64	0.46	-0.81	-18.90	-2.63	-4.97
	UIB-Central	**2.19**	1.81	2.02	-0.84	6.89	-18.08	***-43.79***	-20.20	-4.88	1.05	***4.38***	***2.34***	**2.00**	1.79	-18.34	2.01	-2.47
	Western-Karakoram	1.20	1.00	1.50	***2.00***	0.59	12.09	-4.53	-4.09	**6.40**	***3.50***	***3.82***	***2.03***	***1.88***	1.00	-1.64	***5.43***	2.50
	Karakoram	1.88	2.00	1.33	1.00	-5.82	-7.80	**-64.97**	-37.17	-9.48	0.60	***8.97***	***5.97***	***1.65***	0.11	-24.43	5.64	-3.90
	Hindukush	0.87	0.26	0.15	1.27	2.05	3.49	-6.61	**14.02**	**7.03**	2.17	1.82	1.06	0.75	1.00	3.94	4.44	4.00
	UIB-WU	1.24	**1.02**	1.39	**2.38**	***16.85***	12.38	-25.48	-15.50	-1.28	0.69	0.98	0.52	0.55	***7.76***	-3.68	0.45	-1.25
	Astore	0.05	0.00	0.22	0.50	7.65	4.26	-3.01	5.00	-1.00	-1.11	-0.67	0.00	0.00	2.20	1.97	-0.89	2.16
	Partab_Bridge	1.00	-0.13	3.60	8.80	63.22	-34.86	-39.86	-67.33	29.65	0.69	8.89	15.12	8.40	36.29	-67.00	9.81	-12.40
	UIB-WL	1.88	0.41	6.39	-0.52	41.58	**59.50**	28.19	***81.58***	**30.99**	16.18	5.17	2.33	1.92	19.90	***65.53***	***16.02***	***25.44***
	UIB-WL-Partab	-3.00	0.80	-4.38	-0.82	***87.89***	51.53	9.00	17.67	2.71	-12.24	1.40	-6.00	-3.74	28.32	47.93	-3.00	18.94
	UIB_West	2.45	1.37	5.43	2.42	**61.35**	54.89	0.21	42.93	***28.24***	**13.68**	***5.87***	1.38	2.00	**23.43**	44.18	***17.71***	***22.17***
	Himalaya	0.30	-0.32	4.10	0.91	43.99	62.23	12.43	83.33	22.43	9.97	2.32	0.23	1.17	26.64	**57.88**	7.75	***24.66***
	UIB	1.82	***5.09***	5.37	-2.50	11.35	14.67	-46.60	41.71	35.22	10.17	5.29	0.75	1.91	15.72	-1.40	19.35	4.25

Tabular Figure 6: Results from low altitude stations for the full length of available record (as given in Table 2 and 3) for Tx, Tn, Tavg, DTR and P (rainfall) at monthly to annual time scales in respective units as per Tabular Figures 4 and 5.

Variable	Stations	Jan	Feb	Mar	Apr	May	Jun	Jul	Aug	Sep	Oct	Nov	Dec	DJF	MAM	JJA	SON	Ann.
Tx	Skardu	0.07	0.06	0.06	0.05	0.07	0.02	0.01	0.00	0.02	0.03	0.06	0.06	0.05	0.07	0.01	0.04	0.04
	Astore	0.02	0.01	0.06	0.04	0.05	-0.01	-0.01	-0.02	0.00	0.02	0.03	0.04	0.02	0.06	-0.01	0.02	0.02
	Gupis	0.02	0.02	0.03	0.04	0.06	-0.02	-0.02	-0.03	-0.01	0.04	0.04	0.06	0.04	0.04	-0.02	0.03	0.02
	Gilgit	0.04	0.03	0.04	0.05	0.06	-0.01	-0.01	-0.02	-0.01	0.02	0.05	0.05	0.04	0.04	-0.01	0.02	0.02
	Bunji	0.02	0.01	0.04	0.00	0.01	-0.06	-0.05	-0.05	-0.04	-0.04	0.03	0.02	0.02	0.02	-0.05	-0.02	0.00
	Chilas	-0.01	-0.01	0.03	0.01	0.02	-0.05	-0.02	-0.02	-0.02	0.00	0.00	0.01	0.00	0.02	-0.03	0.00	0.00
Tn	Skardu	0.00	0.02	0.00	-0.01	-0.01	-0.04	-0.04	-0.04	-0.04	-0.05	-0.02	0.01	0.01	0.00	-0.04	-0.04	-0.02
	Astore	0.02	0.01	0.03	0.03	0.04	0.00	-0.02	-0.02	-0.01	0.00	0.02	0.01	0.01	0.04	-0.01	0.01	0.01
	Gupis	-0.04	-0.02	-0.01	-0.03	-0.01	-0.07	-0.06	-0.07	-0.05	-0.03	-0.03	-0.01	-0.03	-0.02	-0.07	-0.05	-0.04
	Gilgit	0.00	0.03	0.00	-0.01	0.01	-0.02	-0.05	-0.03	-0.01	-0.02	-0.01	0.01	0.01	0.00	-0.03	-0.02	-0.01
	Bunji	0.01	0.01	0.03	0.00	0.00	-0.03	-0.04	-0.03	-0.03	-0.03	0.00	0.01	-0.01	0.01	-0.04	-0.04	0.00
	Chilas	0.04	0.02	0.01	0.01	0.03	-0.02	-0.01	-0.03	-0.02	0.00	0.03	0.04	0.03	0.02	-0.02	0.00	0.01
Tavg	Skardu	0.03	0.04	0.03	0.02	0.03	-0.01	-0.02	-0.02	-0.01	0.00	0.02	0.03	0.03	0.03	-0.02	0.00	0.01
	Astore	0.02	0.01	0.04	0.04	0.05	0.00	-0.01	-0.02	0.00	0.01	0.03	0.02	0.01	0.05	-0.01	0.02	0.01
	Gupis	0.00	0.00	0.00	0.01	0.03	-0.04	-0.05	-0.05	-0.03	0.00	0.01	0.02	0.00	0.01	-0.04	-0.01	-0.01
	Gilgit	0.02	0.03	0.02	0.02	0.04	-0.02	-0.03	-0.03	-0.02	-0.01	0.03	0.03	0.03	0.02	-0.03	0.00	0.00
	Bunji	0.00	0.01	0.02	-0.01	-0.01	-0.04	-0.05	-0.04	-0.05	-0.04	0.00	0.01	0.01	0.01	-0.04	-0.03	0.00
	Chilas	0.02	0.00	0.01	0.01	0.03	-0.03	-0.02	-0.02	-0.02	0.00	0.02	0.02	0.01	0.02	-0.03	0.00	0.00
DTR	Skardu	0.06	0.02	0.05	0.07	0.09	0.05	0.06	0.03	0.06	0.09	0.09	0.05	0.05	0.07	0.05	0.09	0.06
	Astore	0.04	0.00	0.01	0.02	0.02	-0.02	0.01	0.02	0.01	0.02	0.02	0.01	0.02	0.01	0.00	0.02	0.02
	Gupis	0.08	0.06	0.05	0.07	0.09	0.06	0.06	0.04	0.07	0.10	0.09	0.08	0.09	0.06	0.05	0.08	0.07
	Gilgit	0.04	0.02	0.04	0.07	0.06	0.00	0.05	0.04	0.05	0.05	0.07	0.05	0.04	0.04	0.03	0.06	0.04
	Bunji	0.04	0.01	0.03	0.01	0.03	0.00	0.00	-0.01	0.03	0.02	0.06	0.04	0.04	0.02	0.00	0.03	0.02
	Chilas	-0.04	-0.02	0.00	0.00	0.00	-0.03	-0.01	0.01	0.01	-0.01	-0.02	-0.03	-0.03	0.00	-0.01	-0.01	-0.02
P	Skardu	0.30	0.32	0.16	0.16	-0.02	0.08	0.06	0.19	0.07	0.00	0.00	0.15	0.98	0.45	0.29	0.12	1.76
	Astore	0.00	-0.28	-0.78	-0.51	-0.25	0.27	0.19	0.06	0.02	-0.05	0.02	-0.08	0.24	-1.31	0.45	0.06	-1.33
	Gupis	0.08	0.04	0.28	0.30	-0.08	0.00	0.24	0.18	0.00	0.00	0.00	0.00	0.11	0.20	0.32	-0.09	2.00
	Gilgit	0.00	0.00	-0.02	0.05	-0.05	0.23	0.01	0.01	0.03	0.00	0.00	0.00	0.02	-0.44	0.28	0.10	0.38
	Bunji	0.00	-0.06	-0.14	0.02	-0.17	0.09	0.05	0.12	0.11	-0.03	0.00	0.00	0.13	-0.59	0.36	0.09	0.21
	Chilas	0.00	0.03	-0.12	0.00	-0.01	0.10	0.07	0.07	0.07	-0.02	0.00	0.00	0.25	-0.12	0.51	0.03	0.70
Q	UIB-East	0.58	0.89	1.18	0.80	0.08	-12.94	-21.37	-10.53	-1.42	-0.18	0.06	0.16	0.55	1.10	-14.86	-0.57	-1.59
	Eastern-Karakoram	0.00	0.00	-0.04	-0.08	1.79	6.46	5.17	6.81	4.34	1.31	0.24	0.00	0.07	0.41	7.08	2.05	2.43
	Central-Karakoram	0.32	-0.07	-0.51	-0.67	6.13	3.85	-1.22	6.30	-7.40	-4.08	-1.36	-0.29	-0.35	1.75	6.22	-2.80	0.31
	Kachura	1.04	1.40	1.19	0.43	6.06	12.88	14.75	19.45	14.27	3.69	1.14	1.13	1.12	2.67	19.20	6.12	7.19
	UIB-Central	0.35	0.21	-0.19	-0.43	9.99	20.49	13.74	20.73	-4.95	-2.15	-0.80	-0.29	-0.30	2.76	17.69	-2.84	3.30
	Western-Karakoram	0.04	0.00	0.00	0.00	0.29	-3.75	-12.69	-13.75	-2.14	-0.24	0.18	0.20	0.13	0.24	-10.23	-0.59	-2.55
	Karakoram	0.28	-0.20	-0.60	0.33	9.67	24.33	8.29	8.13	-7.57	-2.18	-0.59	0.63	-0.15	4.17	24.39	-4.36	6.44
	Hindukush	0.00	0.05	0.04	0.19	3.31	-1.00	-0.85	0.11	0.64	0.23	0.15	0.13	0.04	1.25	0.24	0.31	0.48
	UIB-WU	0.58	0.60	0.33	0.51	3.55	-1.86	-12.74	-12.50	0.68	1.48	1.02	0.71	0.48	1.30	-6.83	1.22	-0.95
	Astore	0.28	0.24	0.32	0.97	3.52	1.29	-0.62	0.54	0.16	0.28	0.32	0.23	0.31	1.63	0.43	0.28	0.76
	Partab_Bridge	1.01	0.49	0.44	1.93	18.03	13.07	12.89	-8.37	9.74	3.84	2.61	1.63	1.74	6.84	7.05	4.93	4.72
	UIB-WL	1.94	1.96	3.49	0.17	2.89	-12.90	-25.95	-12.06	-1.35	1.57	1.94	2.35	1.92	1.93	-13.82	0.48	-2.63
	UIB-WL-Partab	1.58	1.87	2.11	-0.82	-0.30	-22.26	-16.35	-17.07	0.02	-2.20	0.23	1.18	1.32	0.34	-22.10	-0.99	-5.40
	UIB_West	2.02	2.01	2.73	1.12	8.00	-19.88	-32.88	-23.24	-5.13	1.95	2.59	2.40	2.18	3.99	-25.21	0.93	-4.03
	Himalaya	3.23	3.91	4.73	2.33	-0.33	-32.29	-69.33	-17.55	-4.61	-0.05	3.40	2.05	3.37	6.86	-40.09	-0.72	-6.13
	UIB	3.00	3.33	3.53	0.62	12.97	-8.84	-13.31	-3.24	8.19	4.03	3.92	3.04	3.04	5.00	-6.15	5.14	2.23

Tabular Figure 7: Field significance of the climatic trends for all regions considered along with trend in their Q at monthly to annual time scales over the period 1995-2012. Color scale as in Tabular Figure 5.

Regions	Variables	Jan	Feb	Mar	Apr	May	Jun	Jul	Aug	Sep	Oct	Nov	Dec	DJF	MAM	JJA	SON	Ann.
Astore	Tx	-0.17									-0.21		-0.42	-0.16				-0.06
	Tn							-0.10			-0.10		-0.12				-0.10	
	Tavg	-0.15						-0.13			-0.21							-0.05
	DTR		-0.22							-0.13			-0.17	-0.07			-0.06	-0.08
	P			-3.73	-7.50	-4.60	-2.18	-1.90	-1.80	-2.11					-19.25	-6.02	-18.93	-38.01
	Q	0.05	0.00	0.22	0.50	7.65	4.26	-3.01	5.00	-1.00	-1.11	-0.67	0.00	0.00	2.20	1.97	-0.89	2.16
Hindukush	Tx		-0.11	0.23				-0.19		-0.29			-0.18				-0.12	-0.09
	Tn								0.25	0.24		-0.18	-0.24			0.09	0.10	
	Tavg			0.18				-0.11	0.08	-0.25			-0.13				-0.10	
	DTR	-0.21		-0.11	-0.18	-0.25	-0.28	-0.19	-0.36	-0.40	-0.52	-0.38		0.03	-0.16	-0.18	-0.33	-0.20
	P	1.30		-1.94				1.00		1.05	0.31		1.31	4.73	-10.19	-9.80	2.39	
	Q	0.87	0.26	0.15	1.27	2.05	3.49	-6.61	**14.02**	**7.03**	2.17	1.82	1.06	0.75	1.00	3.94	4.44	4.00
Himalaya	Tx	-0.17	-0.10					-0.22		-0.21	-0.19		-0.28	-0.16		-0.07	-0.12	-0.06
	Tn		-0.23	0.26			-0.14	-0.15	0.18		-0.16	-0.18	-0.14	-0.18		-0.13	-0.14	0.02
	Tavg	-0.15		0.25				-0.18	0.17	-0.18	-0.18	-0.09	-0.08	-0.11		-0.10	-0.13	-0.07
	DTR	-0.02	-0.20	0.18	-0.18			-0.13	-0.18	-0.36	-0.25			-0.12		-0.08	-0.19	-0.09
	P			-2.29	-5.71	-4.60	-2.18	-1.90	-1.80	-2.11			0.42		-12.15	-6.02	-18.93	-38.01
	Q	0.30	-0.32	4.10	0.91	43.99	62.23	12.43	83.33	22.43	9.97	2.32	0.23	1.17	26.64	**57.88**	7.75	***24.66***
West Karakoram	Tx			0.23				-0.18		-0.17	-0.16			-0.06				
	Tn		0.22	0.13				-0.13						0.17				0.05
	Tavg	-0.15		0.22	-0.09			-0.14		-0.15								
	DTR		-0.22							-0.13			-0.17	-0.07			-0.06	-0.08
	P					1.17	1.09						3.81	9.08				
	Q	1.20	1.00	1.50	***2.00***	0.59	12.09	-4.53	-4.09	**6.40**	***3.50***	***3.82***	***2.03***	***1.88***	1.00	-1.64	***5.43***	2.50
Karakoram	Tx		-0.11	0.23				-0.18		-0.22	-0.16			-0.06			-0.12	-0.06
	Tn		-0.11	0.23				-0.18		-0.22	-0.16			-0.06			-0.12	-0.06
	Tavg		0.22	0.13			-0.14	-0.14	0.25	0.46	-0.16	-0.18	-0.16	0.17		-0.08	0.06	-0.05
	DTR	-0.15		0.22	-0.09			-0.15	0.08	-0.16	-0.12	-0.09				-0.13	-0.14	-0.08
	P		2.95	1.97		1.17	1.72		1.58	2.15	1.43	2.40	2.69	6.39		5.39	5.76	45.07
	Q	1.88	2.00	1.33	1.00	-5.82	-7.80	***-64.97***	-37.17	-9.48	0.60	***8.97***	***5.97***	***1.65***	0.11	-24.43	5.64	-3.90
UIB Central	Tx							-0.26		-0.20	-0.16						-0.12	
	Tn			0.26			-0.14	-0.20			-0.16	-0.18	-0.16			-0.17	-0.18	0.02
	Tavg			0.25				-0.20		-0.18	-0.15	-0.09				-0.13	-0.14	-0.08
	DTR	0.13										0.09						
	P		2.95	1.97			2.35		1.58	2.15	1.43	2.40	1.57	5.99		5.39	5.76	45.07
	Q	**2.19**	1.81	2.02	-0.84	6.89	-18.08	***-43.79***	-20.20	-4.88	1.05	***4.38***	***2.34***	**2.00**	1.79	-18.34	2.01	-2.47
UIB	Tx	-0.14	-0.11	0.40				-0.20		-0.22	-0.20		-0.25			-0.09	-0.12	-0.09
	Tn		0.49	0.38				-0.13	0.31				-0.17			0.37	-0.14	0.27
	Tavg			0.37				-0.15	0.13	-0.18	-0.16		-0.11			-0.10	-0.12	-0.08
	DTR		-0.19		-0.14			-0.17	-0.24	-0.25	-0.38			0.11	-0.13	-0.10	-0.17	-0.09
	P			-2.17		1.17	-1.42		-2.40	1.65	1.10		1.97	5.98	-11.49	-7.91	3.68	
	Q	1.82	***5.09***	5.37	-2.50	11.35	14.67	-46.60	41.71	35.22	10.17	5.29	0.75	1.91	15.72	-1.40	19.35	4.25
UIB West	Tx	-0.14	-0.11	0.23				-0.18		-0.22	-0.21		-0.25	-0.11		-0.09	-0.12	-0.10
	Tn							-0.12	0.22				-0.18				-0.13	
	Tavg	-0.15		0.20				-0.13	0.13	-0.19	-0.19		-0.11				-0.11	-0.07
	DTR	-0.18	-0.20	-0.10	-0.16			-0.17	-0.24	-0.27	-0.38			-0.10	-0.13	-0.10	-0.19	-0.10
	P			-2.17	-5.71	1.17			-2.40	1.40			1.71	6.90	-11.49	-7.91	2.63	
	Q	2.45	1.37	5.43	2.42	**61.35**	54.89	0.21	42.93	***28.24***	**13.68**	***5.87***	1.38	2.00	**23.43**	44.18	***17.71***	***22.17***
UIB West Lower	Tx	-0.17	-0.10					-0.16		-0.21	-0.20		-0.28	-0.16		-0.07	-0.13	-0.06
	Tn		-0.23					-0.10	0.18				-0.12	-0.18		-0.08	-0.12	
	Tavg	-0.15						-0.13	0.17		-0.19		-0.07	-0.11		-0.06	-0.11	-0.07
	DTR	-0.15	-0.20	0.18	-0.18			-0.13	-0.18	-0.36	-0.25			-0.12		-0.08	-0.19	-0.09
	P			-2.29	-5.71	-4.60	-2.18	-1.90	-1.80	-2.11			0.42		-12.15	-6.02	-18.93	-38.01
	Q	1.88	0.41	6.39	-0.52	41.58	**59.50**	28.19	***81.58***	**30.99**	16.18	5.17	2.33	1.92	19.90	***65.53***	***16.02***	***25.44***
UIB West Upper	Tx	-0.14	-0.11	0.23				-0.18		-0.22	-0.21		-0.25	-0.11		-0.09	-0.12	-0.10
	Tn		0.22	0.13				-0.13	0.25	0.24		-0.18	-0.24	0.17		0.09	0.10	0.05
	Tavg	-0.15		0.20	-0.09			-0.13	0.08	-0.20			-0.13				-0.10	
	DTR	-0.21	-0.22	-0.11	-0.18	-0.25	-0.28	-0.19	-0.36	-0.28	-0.52	-0.38	-0.17	0.06	-0.16	-0.11	-0.19	-0.11
	P	1.30		-1.94		1.17	1.09	1.00		1.40	0.31		2.14	6.90	-10.19	-9.80	2.63	
	Q	1.24	**1.02**	1.39	**2.38**	***16.85***	12.38	-25.48	-15.50	-1.28	0.69	0.98	0.52	0.55	***7.76***	-3.68	0.45	-1.25

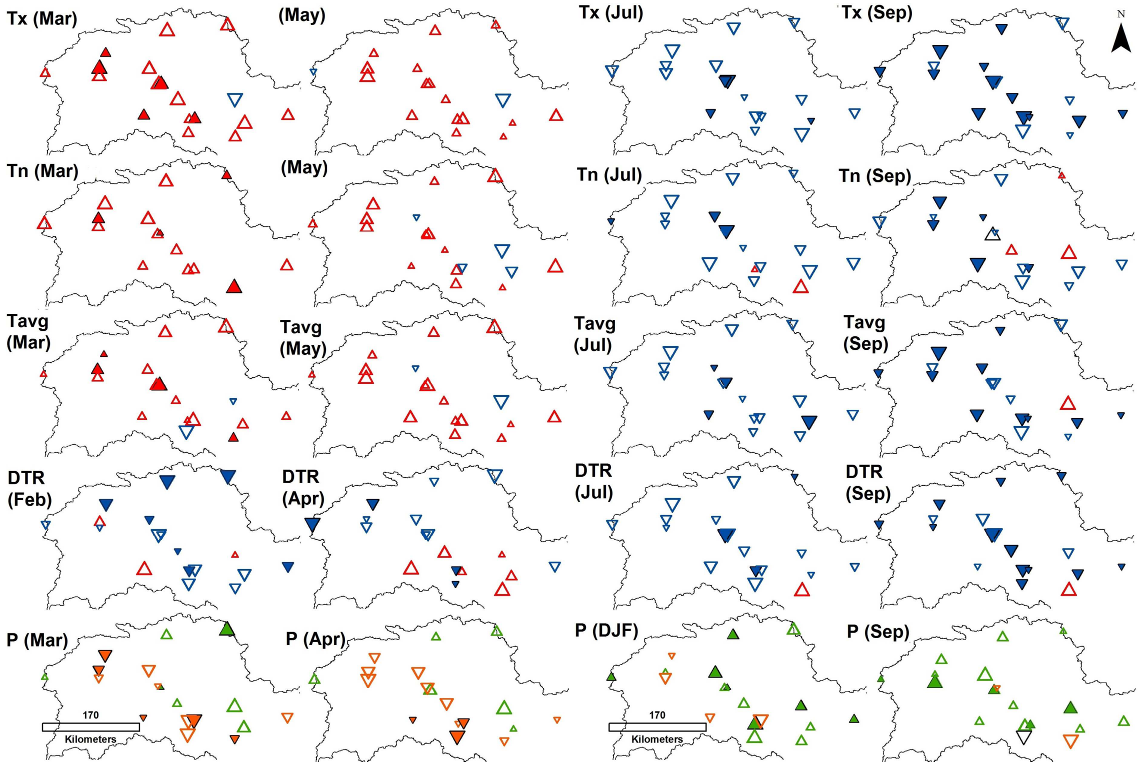

Figure 8: Trend per time step of cooling (downward) and warming (upward) in Tx, Tn and Tavg, and increase (upward) and decrease (downward) in DTR and in P for select months and seasons. Statistically significant trends at ≥ 90% level are shown in solid triangle, the rest in hollow triangles.

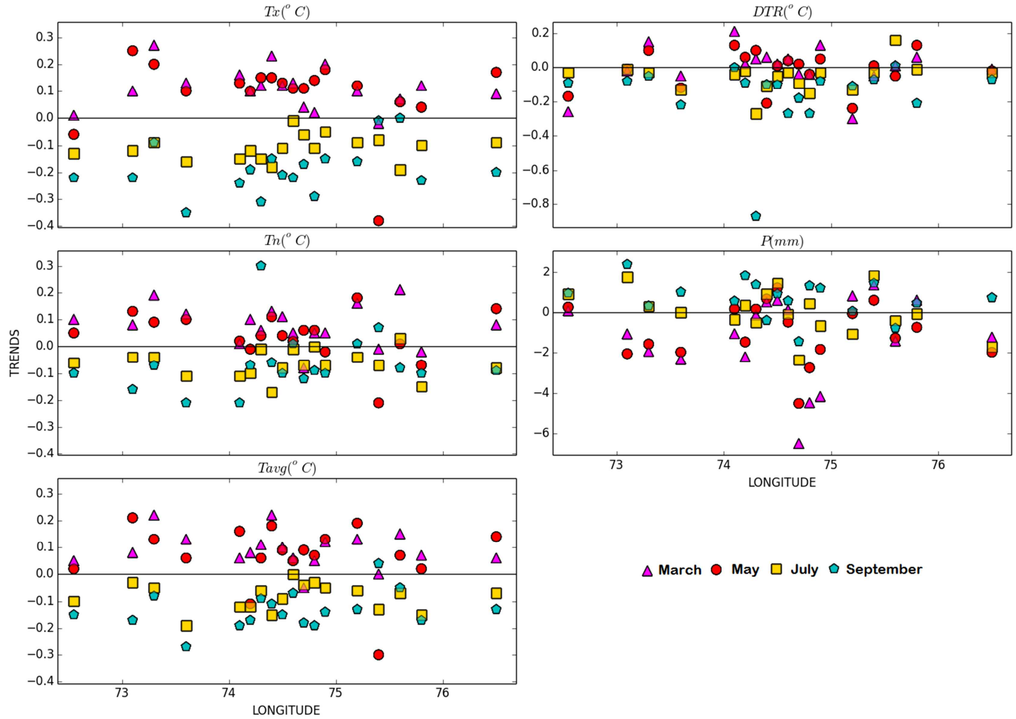

Figure 9: Hydroclimatic trends per unit time for the period 1995-2012 against longitude.

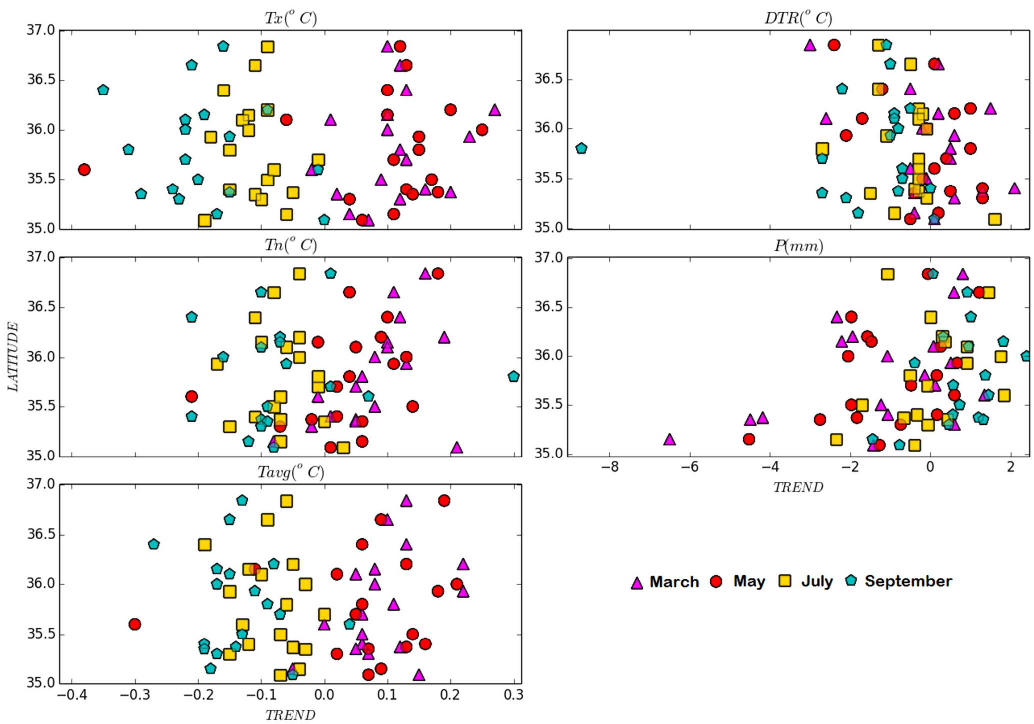

Figure 10: Hydroclimatic trends per unit time for the period 1995-2012 against latitude. Here for DTR only overall trend changes over the whole 1995-2012 period are shown.

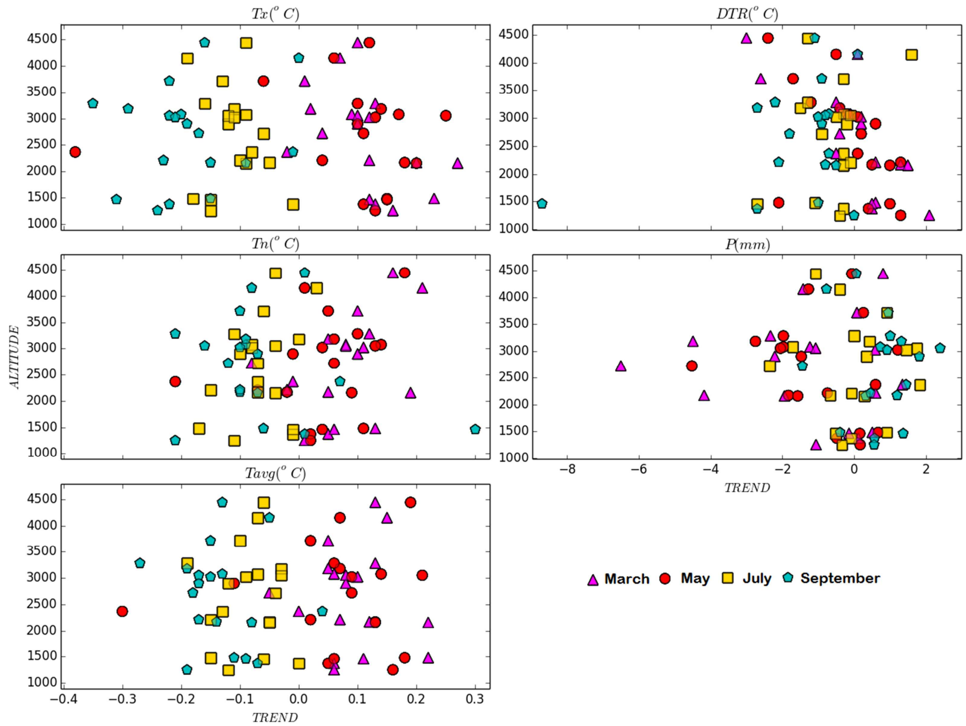

Figure 11: Same as Figure 6 but against altitude.